Postprint of: Malikan, M., Eremeyev, VA, On a flexomagnetic behavior of composite structures, INTERNATIONAL JOURNAL OF ENGINEERING SCIENCE, Vol. 175 (2022), 103671, DOI: 10.1016/j.ijengsci.2022.103671

On a flexomagnetic behavior of composite structures

Mohammad Malikan [1]*, Victor A. Eremeyev [1, 2]

[1] Department of Mechanics of Materials and Structures, Faculty of Civil and Environmental Engineering, Gdańsk University of Technology, ul. Gabriela Narutowicza 11/12, 80-233 Gdańsk, Poland

[2] DICAAR, Università degli Studi di Cagliari, Via Marengo, 2, 09123, Cagliari, Italy

* Correspondence: mohammad.malikan@yahoo.com, mohammad.malikan@pg.edu.pl

Abstract

The popularity of the studies is getting further on the flexomagnetic (FM) response of nano-electro-magneto machines. In spite of this, there are a few incompatibilities with the available FM model. This study indicates that the accessible FM model is inappropriate when considering the converse magnetization effect that demonstrates the necessity and importance of deriving a new FM relation. Additionally, the literature has neglected the converse FM coefficient in the Lifshitz invariant inside the free energy constitutive relation.

This fact inspires us to endeavor and conduct a new characteristic formulation for static analysis of axially compressed piezomagnetic nanobeams comprising the FM effect. This novel FM model is competent and suitable for various boundary conditions, encompassing analytical, semi-analytical, and numerical solving strategies. However, based on the previous FM equation established with respect to Euler-Bernoulli and Timoshenko beams, the

governing equations are ill-posed due to the corresponding energy density. Despite that, this error will not remain in the finalized equations in the present model by conjecturing a gradient of the magnetic field and a different formulation. Moreover, the inverse FM parameter will appear in the magnetic field relation.

As the literature reported, non-uniform deformed piezomagnetic structures are capable of presenting more outstanding flexomagneticity. In actuality, a non-uniform elastic strain appears as a response to the magnetic field gradient (converse effect) that causes this study to deduce the nanobeam with higher-order shear deformations. Furthermore, the local governing equations will be transferred into the nonlocal phase according to the nonlocal differential, particularly nonlocal integral elasticity which itself is a strong nonlocality. Through this theory, and in regard to the converse FM impact, an analytical expression is applied for computing critical buckling loads within several ends conditions of the nanobeam. Our present results and achievements will hopefully be an effective contribution to theoretical studies on the mechanics of intelligent nanostructures.

Keywords: New flexomagnetic model; Higher-order beam; Nonlocal integral theory; Buckling; Analytical solution

1 Introduction

Flexoeffect has been described as a property resulting from electro-magneto-elastic coupling in micro/nano-electro-mechanical systems (MEMS/NEMS) [1, 2]. The appearance of magnetization in relation to the inhomogeneous elastic effect is the most prevalent interpretation of the direct flexoeffect. On the other hand, the effect refers to the emergence of elastic strain in respect to the order parameter gradient. The non-uniform strain or magnetization gradient locally breaks the inversion symmetry of atomic crystalline in spite of centrosymmetry. It is worth noting that flexo-coupling has an impact on both the system's responsiveness to

external stimuli and the inherent gradient of order parameters. The flexomagnetic (FM) effect, which results from the link of the magnetic field with elastic strain gradient (direct effect) and magnetic field gradient with elastic strain (converse effect), is an excellent example in this respect. Materials with non-centrosymmetric crystals have the capability of inducing magnetic potential, and this happens in piezomagnetic materials. Non-uniform shape materials can be constructed by exploiting flexomagneticity, indeed. Regardless of the non-existence of piezomagneticity, such non-uniformity builds large strain gradients and produces magnetism. Notwithstanding, less attention has been merged to the flexomagnetic effect bearing in mind that macroscale is unable to create substantial strain gradients [3-8].

More excitingly, flexomagneticity is an inherently scale-dependent occurrence that can appear extraordinarily in nanoscale in light of the fact that strain gradients are measurably and noticeably manifested in minute sizes. The literature has shown and proven that the manner of deformation has a substantial impact on the behavior of materials due to the scales. First, the rearrangement of the exchange of momentum between bulk boundary space and the free nanoparticles is a prominent process of deformation at the nanoscale. Dislocation motion is a frequent process of deformation at the microscale. Finally, deformation patterning occurs at the macroscale when strain is transferred from one part of the deforming structure to another. On this point, it is necessary to include the size-dependent influences in equilibrium equations of the first two cases causing different material behaviors.

Another kind of generalized continuum theory is nonlocal elasticity. The nonlocal theory integrates points' long-range interactions in a continuum media in terms of physical interpretation. For example, charged molecules or atoms in a solid have this many long-range interactions. Some studies have unveiled that the flexomagnetic response of a nanostructure is influenced by nonlocal effects, and this efficacy is to more distinguished FM effect. On this account, the FM effect can support sensors and actuators in small size very well, resulting in

highly efficient intelligent tools. Eventually, we take care of nonlocal and strain gradient effects in this study for investigating mechanical characteristics of the nanostructure.

There are no vast studies focused on the mechanics of smart structures, including flexomagneticity. Eliseev et al. [7] estimated spontaneously flexoelectric and flexomagnetic as two already known flexoeffect phenomena in nanomaterials. Lukashev and Sabirianov [8] studied the direct flexomagnetic effect using strain gradient tensor by adding additional terms in the free energy expression. In the practical works with physical examples, Sidhardh and Ray [9] investigated the flexomagnetic effect in both inverse and direct flexoeffects for a clamped-free supported (C-F) Euler-Bernoulli beam (thin cantilever beam) based on an exact solution. However, the free energy density function employed in their work *neglected magnetic field gradient and a converse FM parameter* and simply comprised a non-zero strain gradient only. In order to study converse flexoeffect, we seriously need to include a gradient of the magnetic field beside an inverse FM parameter. Their model is well-consistent for a direct flexomagnetic effect. Even though they attempted to make conflict direct and reverse FM effects utilizing dissimilar magnetic boundary conditions over the beam surfaces, their model does not include a converse FM parameter in it. The deflection equation for the cantilever beam in direct and converse modes only contains a direct FM parameter. Zhang et al. [10] followed the model conducted by Sidhardh and Ray and developed it for several exact boundary conditions. Their study clearly shows that *while the converse flexomagnetic effect is analyzed, the FM parameter will vanish in the deflection equation of beams with simply supported-simply supported* (*S-S*), *and clamped-clamped* (*C-C*) *boundary conditions, and lack of any FM coefficients* (*direct or converse*) *is quite apparent*. The deflection relation consisted of a direct FM parameter when using cantilever conditions. It means there is another problem with such the converse FM model. Their direct FM model is totally well-conditioned due to including a direct FM parameter in all boundary conditions. Sladek et al. [11] revised the free energy density for the

direct FM effect by introducing two independent FM parameters. The C-F nanobeam has been investigated by taking into account the Timoshenko assumptions. The prescribed model has been solved by the supposition of exact boundary conditions. Their direct FM model is entirely well-stated, from our knowledge.

Furthermore, in a series of works and a mathematical formalization similar to the two earlier works, Malikan, Eremeyev, and their co-authors studied piezomagnetic-flexomagnetic micro/nanostructures in abundant internal and environmental conditions for various beam and plate-like geometrical shapes [12-23]. All their studies have been performed by means of mathematical modelling, and the models have been solved using analytical, numerical, and semi-analytical solutions. The basic energy relation utilized by them has also been taken from Sidhardh and Ray's work. However, all their published works have solely been done for the converse FM effect. Except for the many valuable findings they obtained, their models had also eliminated any FM parameter in the final governing equations as same as Zhang et al. even when they solved numerically and semi-analytically, the C-C, C-S, C-F, and S-S end conditions. However, in some works, the FM parameter existed in the equilibrium equations [20, 21]. This may reveal that analytical and numerical solving methods can be inconsistent for the reverse flexomagnetic model derived by Sidhardh and Ray. What can be concluded from the above-explained literature is that the available FM model is proper for a direct FM effect while the exact solution is applied.

This work will conquer the two mentioned discussable issues found in the literature. First, we will derive a new energy density function in which the gradient of the magnetic field will appear and exist. By doing this, a converse FM parameter becomes visible in the constitutive equations. Moreover, from the authors of this paper's point of view, the second issue might not relate to boundary conditions' type or solution technique. This problem is hidden in the deformation and displacement fields. Actually, we have tested many conditions to realize when

the FM parameter can remain in the final governing equations. We noticed that if the axial strain is inhomogeneous and non-uniform, both direct and converse FM parameters can stay in the final equations no matter which type of solution has been accomplished. Such a non-uniform strain can be generated on the basis of geometrical or material compositions. The first case can employ a higher-order shear deformation effect in the beam model. On the other side, the second case can be, for example, assuming inhomogeneous composite such as functionally graded structures [20, 21].

The paper's layout follows the next framework. It starts via the second section; we will derive the mathematical models. Section 2.1 is dedicated to showing the previous FM model and its error. Section 2.2 presents the new thermodynamic potential for the general flexomagneticity. In addition, section 2.3 will transfer the model into a nonlocal phase based on the integral (section 2.3.1) and differential (2.3.2) types of nonlocal elasticity. The third section demonstrates an analytical solution process counting several boundary conditions. Further, section 4 validates the solution process. By section 5, the computable results are going to be attained in a comprehensive consideration. The sixth and last section will gather the achievements of this study point by point.

2 Mathematical modelling

Consider a cubic-like composite beam at the *x*-*z* coordinate system that occupies a volume of $[0, L_x]\times[-0.5h, 0.5h]$ (Figure 1). The represented beam is settled in a transverse magnetic field which varies linearly through the thickness dimension.

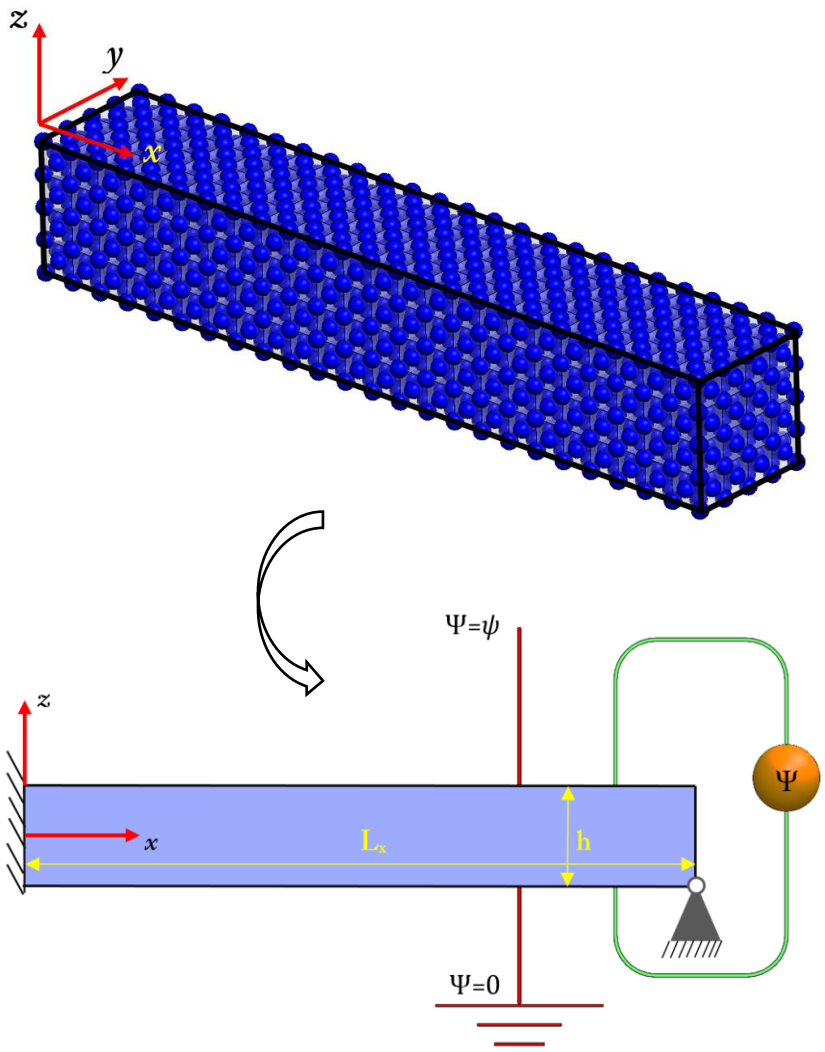

Figure 1 A rectangular continuum meta beam deployed in a magnetic field

2.1 Previous FM model

Running after [9, 10], let summarily review the available mathematical modelling for FM structures. The model is restricted by an initial isothermal condition and minute deformations. The first-order magnetic field tensor (H) and displacement (u) variables are depicted by vector values forms.

$$u = u(x),\ H = H(x) \tag{1}$$

in which we defined x as a position vector.

In the next, the free energy density of the FM model is expressed as [9],

$$\Re_1 = \Re_1(\varepsilon, \eta, H) = -\frac{1}{2} H \cdot a \cdot H + \frac{1}{2} \varepsilon : C : \varepsilon + \frac{1}{2} \eta \vdots g \vdots \eta + \varepsilon : r \vdots \eta \\ -H \cdot q : \varepsilon - H \cdot f \vdots \eta \tag{2}$$

and the variables demonstrated in Eq. (2) are developed as,

Elastic strain: $\varepsilon = \frac{1}{2}\left(\nabla u + \nabla u^T\right)$ (3a)

Strain gradient: $\eta = \nabla \varepsilon$ (3b)

In addition to these, the fourth-order elasticity tensor (*C*), third-order piezomagnetic tensor (*q*), the sixth-order strain gradient tensor (*g*), the fourth-order *direct* flexomagnetic tensor (*f*), the second-order magnetic permeability tensor (*a*), and the fifth-order strain-strain gradient coupling tensor (*r*) are shown. Moreover, "·", ":", and "⋮" stand for scalar (inner) products in spaces of vectors, second-order and third-order tensors, respectively. Finally, let us note that ∇ denotes the 3D nabla operator.

It is worthy to remind that no one can find the gradient of the magnetic field in Eq. (2).

The magnetic potential (ψ) can be formulated with the magnetic field as,

$$H = -\nabla \psi \tag{4}$$

The characteristic equation for the flexomagnetic structures in the static conditions can be derived based on the variational principle as,

$$\delta \int_V U dV = \delta W \tag{5}$$

in which *W* means the work of external forces, and *V* defines the domain's volume. Moreover, the first variation of free energy (here, strain energy (*U*)) over the volume *V* has been written for free energy density.

It is now supposed that,

$$\delta W = \int_V F \cdot \delta u + \int_{\partial V} t \cdot \delta u ds \tag{6}$$

in which the surface traction and external mass loads are revealed by *t* and *F*, respectively.

Let us apply the calculus of variational technique to obtain the max and min of Eq. (5) as

$$\nabla \cdot \left(\sigma - \nabla \cdot \xi \right) + F = 0 \tag{7a}$$

$$\nabla \cdot B = 0 \tag{7b}$$

where the first-order magnetic flux tensor has been associated with *B*.

Let now introduce the constitutive relations in the following,

$$\sigma = \frac{\partial \Re_1}{\partial \varepsilon} = C : \varepsilon + r \vdots \eta - H \cdot q \tag{8a}$$

$$\xi = \frac{\partial \Re_1}{\partial \eta} = g : \eta + \varepsilon : r - H \cdot f \tag{8b}$$

$$B = -\frac{\partial \Re_1}{\partial H} = a \cdot H + q : \varepsilon + f \vdots \eta \tag{8c}$$

We expand the above relations by considering relatively thick beams respecting non-uniform shear deformation assumptions generating the non-uniform axial strain. For this purpose, the following displacement field is investigated [24]

$$u_1(x,z) = -z\frac{dw}{dx} + f(z)\phi(x) \tag{9a}$$

$$u_3(x,z) = w(x) \tag{9b}$$

where using the Reddy function $f(z) = z\left(1-4z^2/3h^2\right)$ leads to a higher-order shear deformation beam.

Having found the elastic strains using linear Lagrangian strain, we proceed to find hyper strain as well [25-27],

$$\varepsilon_{ij} = \frac{1}{2}\left(\frac{\partial u_i}{\partial x_j} + \frac{\partial u_j}{\partial x_i}\right) \tag{10}$$

Then,

$$\varepsilon_{xx} = -z\frac{d^2w}{dx^2} + f(z)\frac{d\phi}{dx} \tag{11a}$$

$$\gamma_{xz} = f'(z)\phi \tag{11b}$$

$$\eta_{xxz} = \frac{d\varepsilon_{xx}}{dz} = -\frac{d^2w}{dx^2} + f'(z)\frac{d\phi}{dx} \tag{11c}$$

where the prime $(\ )'$ means the first derivative with respect to *z*.

Letting alone the three-dimensional flexomagnetic characteristics equations, the one-dimensional FM relations can be displayed below,

$$\sigma_{xx} = C_{11}\varepsilon_{xx} - q_{31}H_z \tag{12a}$$

$$\tau_{xz} = G\gamma_{xz} \tag{12b}$$

$$\xi_{xxz} = g_{31}\eta_{xxz} - f_{31}H_z \tag{12c}$$

$$B_z = a_{33}H_z + q_{31}\varepsilon_{xx} + f_{31}\eta_{xxz} \tag{12d}$$

It is now expected to find equilibrium equations and non-classical boundary conditions by doing Eq. (13),

$$\delta\left(U + W\right) = 0 \tag{13}$$

where

$$\delta U = \int_V \left(\sigma_{xx}\delta\varepsilon_{xx} + \tau_{xz}\delta\gamma_{xz} + \xi_{xxz}\delta\eta_{xxz} - B_z\delta H_z\right)dV \tag{14}$$

Having applied the variational technique gives us the governing equations and connected boundary conditions parts by parts as,

$$\delta U = \delta U_1^{Mech} + \delta U_1^{Mag} + \delta U_2^{Mech} + \delta U_2^{Mag} \tag{15}$$

where

$$\delta U_1^{Mech} = \int_0^{L_x}\left[\left(\frac{d^2M_x}{dx^2} + \frac{d^2T_{xxz}}{dx^2}\right)\delta w + \left(Q_x - \frac{dV_x}{dx} - \frac{dR_x}{dx}\right)\delta\phi\right]dx \tag{16a}$$

$$\delta U_2^{Mech} = \left[-\frac{d}{dx}\left(\left(M_x + T_{xxz}\right)\delta w\right) + \left(V_x + R_x\right)\delta\phi\right]_0^{L_x} \tag{16b}$$

$$\delta U_1^{Mag} = -\int_0^{L_x}\int_{-h/2}^{h/2}\frac{dB_z}{dz}\delta\Psi\,dz\,dx \tag{16c}$$

$$\delta U_2^{Mag} = \int_0^{L_x} \left(B_z \delta \Psi \right) \Big|_{-h/2}^{h/2} dx \tag{16d}$$

The parameters involved in Eq. (16) are stress resultants embracing the bending moment and hyper stress as follows,

$$M_x = \int_{-h/2}^{h/2} z \sigma_{xx} dz \tag{17a}$$

$$V_x = \int_{-h/2}^{h/2} f\left(z\right) \sigma_{xx} dz \tag{17b}$$

$$Q_x = \int_{-h/2}^{h/2} f'\left(z\right) \tau_{xz} dz \tag{17c}$$

$$T_{xxz} = \int_{-h/2}^{h/2} \xi_{xxz} dz \tag{17d}$$

$$R_x = \int_{-h/2}^{h/2} f'\left(z\right) \xi_{xxz} dz \tag{17e}$$

Let remind the equation defining connectivity between magnetic field component and magnetic potential as follows,

$$\frac{d\Psi}{dz} + H_z = 0 \tag{18}$$

The magnetic force transferred from lateral magnetic field appeared on both ends, and this force produces thermodynamic work on the system as,

$$\delta W = \int_0^{L_x} N_x^0 \left(\frac{d\delta w}{dx} \frac{dw}{dx} \right) dx \tag{19}$$

The discussion continues by determining the magnetic potential values on the external top and bottom surfaces of the beam [9],

$$\Psi\left(+\frac{h}{2}\right)=\psi \tag{20a}$$

$$\Psi\left(-\frac{h}{2}\right)=0 \tag{20b}$$

Roughly speaking, let us assume that the magnetic potential changes linearly according to the following hypothesis in the lateral dimension and varies through the length. By these assumptions, a closed-circuit condition can also be deemed. Besides, the spatial magnetic potential, which relates to the variation of the magnetic potential in line with the length, is here a variable of deflection. We are now able to devote the expression for magnetic potential through thickness and length of the beam by means of Eqs. (12d), (16c), (18), and (20),

$$\Psi=-\frac{q_{31}}{a_{33}}\left[\left(\frac{z^2}{2}-\frac{h^2}{8}\right)\frac{d^2w}{dx^2}-\left(\frac{z^2}{2}-\frac{z^4}{3h^2}-\frac{5h^2}{48}\right)\frac{d\phi}{dx}\right]+\frac{f_{31}}{3a_{33}}\left(z-\frac{4z^3}{h^2}\right)\frac{d\phi}{dx}+\frac{\psi}{h}\left(z+\frac{h}{2}\right) \tag{21}$$

As easily seen, Eq. (21) can be satisfied by suppositions made in Eq. (20), but *it excludes the converse FM effect*, which, in turn, cannot be a well-posedness model. Indeed, Eq. (20) is the magnetic conditions for the inverse magnetic effect; however, as Eq. (2) did not contain any reverse FM impact, so then Eq. (21) is derived in an unwell state.

Eq. (21) can be derived based on the $\Psi\left(\pm h/2\right)=\psi$ consistent for a direct FM model. Later, Eq. (22) stems from Eqs. (18) and (21),

$$H_z=z\frac{q_{31}}{a_{33}}\frac{d^2w}{dx^2}-\left[\frac{q_{31}}{a_{33}}f\left(z\right)+\frac{f_{31}}{3a_{33}}\left(3f'\left(z\right)-2\right)\right]\frac{d\phi}{dx}-\frac{\psi}{h} \tag{22}$$

Thereafter, Eq. (12) becomes extracted by accessing Eq. (11), and (22),

$$\sigma_{xx} = -\left[z\frac{q_{31}^2}{a_{33}}\frac{d^2w}{dx^2} - \left(\frac{q_{31}^2}{a_{33}} f(z) + \frac{q_{31}f_{31}}{3a_{33}}\left(3f'(z)-2\right)\right)\frac{d\phi}{dx}\right] + C_{11}\left(f(z)\frac{d\phi}{dx} - z\frac{d^2w}{dx^2}\right) + \frac{q_{31}\psi}{h} \tag{23a}$$

$$\tau_{xz} = Gf'(z)\phi \tag{23b}$$

$$\xi_{xxz} = g_{31}\left(f'(z)\frac{d\phi}{dx} - \frac{d^2w}{dx^2}\right) + \left[\frac{f_{31}q_{31}}{a_{33}} f(z) + \frac{f_{31}^2}{3a_{33}}\left(3f'(z)-2\right)\right]\frac{d\phi}{dx} - z\frac{f_{31}q_{31}}{a_{33}}\frac{d^2w}{dx^2} + \frac{\psi f_{31}}{h} \tag{23c}$$

$$B_z = zq_{31}\frac{d^2w}{dx^2} - \left[q_{31}f(z) + \frac{f_{31}}{3}\left(3f'(z)-2\right)\right]\frac{d\phi}{dx} + q_{31}\left(f(z)\frac{d\phi}{dx} - z\frac{d^2w}{dx^2}\right) + f_{31}\left(f'(z)\frac{d\phi}{dx} - \frac{d^2w}{dx^2}\right) - \frac{\psi a_{33}}{h} \tag{23d}$$

And then, Eq. (17) can also be pulled out as,

$$M_x = -\left(I_{11}+I_{12}\right)\frac{d^2w}{dx^2} + \left(I_{13}+I_{14}+I_{15}\right)\frac{d\phi}{dx} \tag{24a}$$

$$Q_x = I_{16}\phi \tag{24b}$$

$$T_{xxz} = -I_{17}\frac{d^2w}{dx^2} + \left(I_{18}+I_{19}+I_{110}\right)\frac{d\phi}{dx} + I_{111} \tag{24c}$$

$$V_x = -\left(I_{13}+I_{14}\right)\frac{d^2w}{dx^2} + \left(I_{112}+I_{113}+I_{114}\right)\frac{d\phi}{dx} + I_{115} \tag{24d}$$

$$R_x = -\left(I_{15}+I_{18}\right)\frac{d^2w}{dx^2} + \left(I_{116}+I_{117}+I_{118}\right)\frac{d\phi}{dx} + I_{119} \tag{24e}$$

where letters in Eq. (24) can be rescripted by Appendix A,

The strain gradient part (g_{31}) is also an unknown variable; however, one can have the benefit of the availability of the given generalized first strain theory of elasticity [28]. Subsequently, by introducing an internal length parameter for the material, the strain gradient elasticity tensor will be simplified,

$$\begin{aligned} g_{jklmni} &= g_1\left[\left(\delta_{ij}\delta_{kl}+\delta_{ik}\delta_{jl}\right)\delta_{mn}+\left(\delta_{im}\delta_{ln}+\delta_{in}\delta_{lm}\right)\delta_{jk}\right] \\ &+g_2\left[\delta_{ij}\left(\delta_{km}\delta_{ln}+\delta_{kn}\delta_{lm}\right)+\delta_{ik}\left(\delta_{jm}\delta_{ln}+\delta_{jn}\delta_{lm}\right)\right]+g_3\delta_{il}\delta_{jk}\delta_{mn} \\ &+g_4\delta_{il}\left(\delta_{jm}\delta_{kn}+\delta_{jn}\delta_{km}\right)+g_5\left[\delta_{im}\left(\delta_{jn}\delta_{kl}+\delta_{jl}\delta_{kn}\right)+\delta_{in}\left(\delta_{jm}\delta_{kl}+\delta_{jl}\delta_{km}\right)\right] \end{aligned} \tag{25}$$

where c_{klmn} means elasticity modulus, δ_{li} denotes Kronecker delta, and l is being a material length scale parameter (SGLS). The g_i would be,

$$\begin{aligned} &g_1=-\frac{2}{3}\left(g_2+g_5\right),\ g_2=\frac{G}{30}\left(27l_0^2-4l_1^2-15l_2^2\right) \\ &g_3=\frac{1}{3}\left(8g_2+2g_5\right),\ g_4=\frac{G}{3}\left(l_1^2+6l_2^2\right),\ g_5=\frac{G}{3}\left(l_1^2-3l_2^2\right). \end{aligned} \tag{26}$$

We assume that $l_0=l_1=l_2=l$. Moreover, the heretofore used strain gradient hypothesis lacks the required literature in order to evaluate the shear modulus $\left\{G=C_{11}/2\left(1+\nu\right)\right\}$, which is a scalar.

It is already known that,

$$\delta_{ij}=\begin{cases}1, & if\ \ i=j,\\ 0, & if\ \ i\neq j.\end{cases} \tag{27}$$

Therefore, $g_{jklmni}=g_{311311}=g_{31}$. Then,

$$g_{31} = g_3 + 2g_4 \tag{28}$$

The variational formulation has so far been performed on the system's energy. Afterward, imposing Eq. (16) brings about the following relations, which are associated with axially buckling of a piezomagnetic-flexomagnetic (PFM) beam,

$$\delta w = 0;\ \frac{d^2 M_x}{dx^2} + \frac{d^2 T_{xxz}}{dx^2} + N_x^0 \frac{d^2 w}{dx^2} = 0 \tag{29a}$$

$$\delta\phi = 0;\ Q_x - \frac{d}{dx}\left(V_x + R_x\right) = 0 \tag{29b}$$

Then, using Eq. (24), one obtains

$$-\left(I_{11} + I_{12} + I_{17}\right)\frac{d^4 w}{dx^4} + \left(I_{13} + I_{14} + I_{15} + I_{18} + I_{19} + I_{110}\right)\frac{d^3\phi}{dx^3} + N_x^0 \frac{d^2 w}{dx^2} = 0 \tag{30a}$$

$$\left(I_{13} + I_{14} + I_{15} + I_{18}\right)\frac{d^3 w}{dx^3} - \left(I_{112} + I_{113} + I_{114} + I_{116} + I_{117} + I_{118}\right)\frac{d^2\phi}{dx^2} + I_{16}\phi = 0 \tag{30b}$$

Irrespective of the solution process, as observed, the converse FM parameter did not appear inside the final equation. Although the model works, it elucidates that the gradient of the magnetic field has been excluded during operating with mathematical modeling. It seems that this model covers a direct FM effect incorporating strain gradient and direct FM tensors, even though the magnetic boundary conditions have been carried out for a converse FM impact. Overall, it can be expressed that this model is in an ill-conditioning posture.

Not to mention that, if $f(z)$ has been eliminated, Eq. (30) diminishes to $\left[\left(I_{11} + I_{12} + I_{17}\right)d^4 w/dx^4 - \left(N_x^0\right)d^2 w/dx^2 = 0\right]$ in which the FM parameter will not exist due to strain uniformity.

2.2 New fundamental FM model

In most recently published scientific articles, the expression for the thermodynamic potential of a PFM system has been expressed similar to Eq. (2). However, this hypothesis can result in the absence of reverse flexomagnetic tensor in the final coupled equations while considering the converse FM effect. Thus, this can be the reasoning for the ill-posedness of the FM model conducted by [9, 10]. In fact, Eq. (2) enables us to consider a direct FM effect only due to having a strain gradient. The magnetic field gradient shall be included in the free energy relation to consider a converse FM effect. Here, we are supposed to add a gradient of the magnetic field in the fundamental free energy density function based on the general form of Lifshitz invariant and modify it as (Note that here we simply use ε_{ij} , H_k and their gradients to develop the free energy relation),

$$\begin{aligned}\Re_2 &= \frac{1}{2}C_{ijkl}\varepsilon_{ij}\varepsilon_{kl} - \frac{1}{2}a_{kl}H_kH_l - q_{ijk}\varepsilon_{ij}H_k + \frac{1}{2}g_{ijklmn}\frac{\partial\varepsilon_{ij}}{\partial x_k}\frac{\partial\varepsilon_{lm}}{\partial x_n} \\ &+ r_{ijklm}\varepsilon_{ij}\frac{\partial\varepsilon_{kl}}{\partial x_m} - \frac{1}{2}b_{ijkl}\frac{\partial H_i}{\partial x_j}\frac{\partial H_k}{\partial x_l} - s_{ijk}H_i\frac{\partial H_j}{\partial x_k} - \lambda_{ijklm}\frac{\partial\varepsilon_{ij}}{\partial x_k}\frac{\partial H_l}{\partial x_m} \\ &- \frac{1}{2}f_{ijkl}\frac{\partial\varepsilon_{ij}}{\partial x_k}H_l - \frac{1}{2}h_{ijkl}\varepsilon_{ij}\frac{\partial H_k}{\partial x_l}\end{aligned} \tag{31}$$

where the employed tensors are defined as,

f_{ijkl} : 4th order *direct* flexomagnetic tensor

h_{ijkl} : 4th order *converse* flexomagnetic tensor

r_{ijklm} : 5th order strain-strain gradient coupling tensor

s_{ijk} : 3rd order magnetic field-magnetic field gradient coupling tensor

λ_{ijklm} : 5th order strain gradient-magnetic field gradient coupling tensor

g_{ijklmn} : 6th order strain gradient tensor

b_{ijkl} : 4th order magnetic field gradients coupling tensor

q_{ijk} : 3rd order piezomagnetic tensor

a_{kl} : 2nd order magnetic permeability tensor

C_{ijkl} : 4th order pure elasticity tensor

This novel equation stands for the general PFM model and has not been already existed in the literature. For example, for centrosymmetric materials, q_{ijk} and λ_{ijklm} are taken to be zero. However, for such materials, f_{ijkl} and h_{ijkl} still exist.

This equation incorporates a magnetic field gradient essential to examining a reverse FM effect. When an external magnetic potential actuates a non-centrosymmetric smart structure, its crystals produce mechanical deformations due to both the magnetic field and its gradient. These phenomena are called converse piezomagnetic (PM) and flexomagnetic (FM) effects. However, when the intelligent structure is mechanically deformed, its crystals will be magnetized and induce an internal short magnetic field. The mechanical strain and its gradient create magnetic potential, called direct PM and FM effects. What is more, according to the literature [9], the difference between direct and converse effects are in magnetic boundary conditions only, which cannot be correct. It means we severely need to involve the magnetic field gradient in the energy density function.

The following new constitutive equations are derived from Eq. (31),

$$\sigma_{ij} = \frac{\partial \Re_2}{\partial \varepsilon_{ij}} = C_{ijkl}\varepsilon_{kl} - q_{ijk}H_k + r_{ijklm}\frac{\partial \varepsilon_{kl}}{\partial x_m} - h_{ijkl}\frac{\partial H_k}{\partial x_l} \tag{32a}$$

$$\tau_{ijk} = \frac{\partial \Re_2}{\partial\left(\frac{\partial \varepsilon_{ij}}{\partial x_k}\right)} = g_{ijklmn}\frac{\partial \varepsilon_{lm}}{\partial x_n} + r_{ijklm}\varepsilon_{ij} - \lambda_{ijklm}\frac{\partial H_l}{\partial x_m} - f_{ijkl}H_l \tag{32b}$$

$$T_{ij} = \frac{\partial \Re_2}{\partial\left(\frac{\partial H_i}{\partial x_j}\right)} = -b_{ijkl}\frac{\partial H_k}{\partial x_l} - s_{ijk}H_i - \lambda_{ijklm}\frac{\partial \varepsilon_{ij}}{\partial x_k} - h_{ijkl}\varepsilon_{ij} \tag{32c}$$

$$B_i = -\frac{\partial \Re_2}{\partial H_i} = a_{kl}H_k + q_{ijkl}\varepsilon_{ij} + s_{ijk}\frac{\partial H_j}{\partial x_k} + f_{ijkl}\frac{\partial \varepsilon_{ij}}{\partial x_k} \tag{32d}$$

There is no available literature presenting a value for r_{ijklm}, s_{ijk}, λ_{ijklm}, and b_{ijkl} tensors for piezomagnetic materials. Henceforward, we have to ignore them for the following formulation. Furthermore, as we are going to study the reverse FM influence only, then we eliminate the direct FM parameter at the end. Let us now simplify Eq. (32) for a one-dimensional beam as

$$\sigma_{xx} = C_{11}\varepsilon_{xx} - q_{31}H_z - h_{31}\frac{dH_z}{dz} \tag{33a}$$

$$\tau_{xz} = G\gamma_{xz} \tag{33b}$$

$$\xi_{xxz} = g_{31}\eta_{xxz} - f_{31}H_z \tag{33c}$$

$$T_{zz} = -h_{31}\varepsilon_{xx} \tag{33d}$$

$$B_z = a_{33}H_z + q_{31}\varepsilon_{xx} + f_{31}\eta_{xxz} \tag{33e}$$

As a consequence, the variation of strain energy density would be

$$\delta U = \int_V \left(\sigma_{xx}\delta\varepsilon_{xx} + \tau_{xz}\delta\gamma_{xz} + \xi_{xxz}\delta\eta_{xxz} - T_z\delta\frac{dH_z}{dz} - B_z\delta H_z \right) dV \tag{34}$$

where

$$\delta U_1^{Mag} = -\int_0^{L_x}\int_{-h/2}^{h/2}\left(\frac{dB_z}{dz}+\frac{d^2T_{zz}}{dz^2}\right)\delta\Psi dzdx \tag{35a}$$

$$\delta U_2^{Mag} = \int_0^{L_x}\left[B_z+\frac{dT_{zz}}{dz}\right]_{-h/2}^{h/2}\delta\Psi dx \tag{35b}$$

Doing precisely the equivalent mathematical efforts required to obtain Eq. (21) but here by means of Eqs. (18), (20), (33e), and (35a), provides,

$$\Psi = -\frac{q_{31}}{a_{33}}\left[\left(\frac{z^2}{2}-\frac{h^2}{8}\right)\frac{d^2w}{dx^2}-\left(\frac{z^2}{2}-\frac{z^4}{3h^2}-\frac{5h^2}{48}\right)\frac{d\phi}{dx}\right]+\frac{1}{3}\left(\frac{f_{31}-h_{31}}{a_{33}}\right)\left(z-\frac{4z^3}{h^2}\right)\frac{d\phi}{dx} + \frac{\psi}{h}\left(z+\frac{h}{2}\right) \tag{36}$$

where Eq. (36) includes *the inverse FM effect*. Moreover, it is obvious that Eq. (36) will not violate the Maxwell general electrostatic equation ($\nabla\times\overline{H}=\left(\frac{\partial H_z}{\partial y}-\frac{\partial H_y}{\partial z}\right)\vec{i}+\left(\frac{\partial H_x}{\partial z}-\frac{\partial H_z}{\partial x}\right)\vec{j}+\left(\frac{\partial H_y}{\partial x}-\frac{\partial H_x}{\partial y}\right)\vec{k}$), and thus it can represent a static magnetic field.

Then, based on Eq. (36), the axial and transverse components of the magnetic field are obtainable as,

$$H_z = z\frac{q_{31}}{a_{33}}\frac{d^2w}{dx^2}-\left[\frac{q_{31}}{a_{33}}f(z)+\frac{1}{3}\left(\frac{f_{31}-h_{31}}{a_{33}}\right)\left(3f'(z)-2\right)\right]\frac{d\phi}{dx}-\frac{\psi}{h} \tag{37}$$

In contrast to the previous FM model, which included a magnetic part in the coupled governing equation [9], the present model contains two dependent equations. By means of Eqs. (11), (33), and (37), local stress and higher-order stresses are expanded as,

$$\sigma_{xx} = -\left[z\frac{q_{31}^2}{a_{33}}\frac{d^2w}{dx^2} - \left(\frac{q_{31}^2}{a_{33}} f(z) + \frac{q_{31}}{3}\left(\frac{f_{31}-h_{31}}{a_{33}} \right)\left(3f'(z)-2\right) \right)\frac{d\phi}{dx} \right]$$
$$+C_{11}\left(f(z)\frac{d\phi}{dx} - z\frac{d^2w}{dx^2} \right) + \frac{q_{31}\psi}{h} - h_{31}\frac{q_{31}}{a_{33}}\frac{d^2w}{dx^2} \tag{38a}$$
$$+h_{31}\left[\frac{q_{31}}{a_{33}} f'(z) + \left(\frac{f_{31}-h_{31}}{a_{33}} \right) f''(z) \right]\frac{d\phi}{dx}$$

$$\xi_{xxz} = g_{31}\left(f'(z)\frac{d\phi}{dx} - \frac{d^2w}{dx^2} \right) + \left[\frac{f_{31}q_{31}}{a_{33}} f(z) + \frac{1}{3} f_{31}\left(\frac{f_{31}-h_{31}}{a_{33}} \right)\left(3f'(z)-2\right) \right]\frac{d\phi}{dx} \tag{38b}$$
$$-z\frac{f_{31}q_{31}}{a_{33}}\frac{d^2w}{dx^2} + \frac{\psi f_{31}}{h}$$

$$T_{zz} = -h_{31}\left(f(z)\frac{d\phi}{dx} - z\frac{d^2w}{dx^2} \right) \tag{38c}$$

At this stage, filling in Eq. (17) with Eq. (38) leads to,

$$M_x = -\left(I_{21}+I_{22}\right)\frac{d^2w}{dx^2} + \left(I_{23}+I_{24}+I_{25}+I_{2110}+I_{2111}\right)\frac{d\phi}{dx} \tag{39a}$$

$$V_x = -\left(I_{23}+I_{24}+I_{2112}\right)\frac{d^2w}{dx^2} + \left(I_{212}+I_{213}+I_{214}+I_{2113}+I_{2114}\right)\frac{d\phi}{dx} + I_{215} \tag{39b}$$

$$Q_x = I_{26}\phi \tag{39c}$$

$$T_{xxz} = -I_{27}\frac{d^2w}{dx^2} + \left(I_{28}+I_{29}+I_{210}\right)\frac{d\phi}{dx} + I_{211} \tag{39d}$$

$$R_x = -\left(I_{28}+I_{2115}\right)\frac{d^2w}{dx^2} + \left(I_{216}+I_{217}+I_{218}\right)\frac{d\phi}{dx} + I_{219} \tag{39e}$$

where the numerical parameters can be found in Appendix B.

It has become quite obvious that substituting the above-mentioned stress resultants into the governing equations (Eq. (29)) will cause the advent of the converse FM parameter inside it.

$$\begin{aligned}&\left(I_{23}+I_{24}+I_{25}+I_{28}+I_{29}+I_{210}+I_{2110}+I_{2111}\right)\frac{d^3\phi}{dx^3}\\&-\left(I_{21}+I_{22}+I_{27}\right)\frac{d^4w}{dx^4}+N_x^0\frac{d^2w}{dx^2}=0\end{aligned}\tag{40a}$$

$$\begin{aligned}&-\left(I_{212}+I_{213}+I_{214}+I_{216}+I_{217}+I_{218}+I_{2113}+I_{2114}\right)\frac{d^2\phi}{dx^2}\\&+\left(I_{23}+I_{24}+I_{28}+I_{2112}+I_{2115}\right)\frac{d^3w}{dx^3}+I_{26}\phi=0\end{aligned}\tag{40b}$$

As flexomagneticity is dominant in nanoscale, it is supposed to develop Eq. (40) on a nanodomain. Then, it is now time to involve the nonlocal effect into the model. Here, the strong form of nonlocality, which means the nonlocal integral elasticity approach of Eringen, will be utilized. To begin with, the constitutive equation of the two phases local/nonlocal integral model can be expressed in the next section.

2.3 Nonlocal phase

Hitherto, all the formulations have been done in local media. Thereafter, the mathematical model will enter the nonlocal phase with respect to Eringen's nonlocal elasticity theory for the homogeneous deformable solid [29]. It is one of the non-classical continuum theories whose characteristic equation is in an integral form. This fundamental equation is assumed to consider the nonlocal effect, the philosophy of discontinuity of the material environment, and consequently, the discontinuity of the mechanical field (stress and strain tensors). In fact, this theory introduces the forces between atoms in a continuous body as an effective parameter to overcome the problems.

In the classical method, when the beams and plates have been examined on a large scale, it is deemed that the distance between the atoms is minimal compared to the object's length, so the effect of the characteristic length on the relations is not considered. However, in the case of nanobeams, due to the small length of the beam, the effect of characteristic length cannot be ignored, and this element enters the mechanical analyses as an influential factor.

The given nonlocal constitutive relation is re-shown as,

$$\sigma_{xx}(x)=\int_0^{L_x} k(|x'-x|,\tau)\left[C_{11}(z)\varepsilon_{xx}(x')-q_{31}(z)H_z(x')-h_{31}(z)\frac{dH_z}{dz}(x')\right]dx' \tag{41}$$

When the nonlocal parameter value reaches zero, the kernel function, which is symmetric regarding *x*, has converged to the Dirac delta. Nonlocal modulus usually meets small values, and the essence of nonlocal theory enables us to draw the atomic lattice dynamics approximately as [30],

$$k^{1D}(|x'-x|,\tau)=\frac{1}{2\tau}\mathrm{e}^{-\frac{|x'-x|}{\tau}} \tag{42}$$

in which τ depicts the nonlocal parameter pertaining to both material constant (e_0), and an internal length scale (a), in the frame $\tau=e_0a$.

Therefore, Eq. (42) can be obtained by merging both local and nonlocal phases, which will be exhibited later.

2.3.1 Nonlocal integral model

In Eringen's theory of nonlocal elasticity, on the material medium, the stress tensor at a point depends on a strain tensor on the whole domain by an integral equation. In other words, the main structural equation of the theory of nonlocal elasticity is expressed integrally [30-41].

The literature underscored some discordances between Eringen's nonlocal differential and integral-types for the case of cantilever beams [35]. Accordingly, it is rigorously proposed to take advantage of the integral model. Hence, the integral elasticity model is here re-structured in local/nonlocal phases by exploiting Eq. (42) as the second kind of Fredholm integral-type theory,

$$t_{xx}(x)=\xi_1\sigma(x)+\frac{\xi_2}{2\tau}\int_0^{L_x}e^{-\frac{|x-s|}{\tau}}\sigma(s)ds \tag{43}$$

where ξ_1 and ξ_2 are weight factors and comply with two material's phases. Their values should satisfy $\xi_1+\xi_2=1$ when $\xi_1\geq 0$ and $\xi_2\geq 0$. In some references, ξ_1 has been ignored. Obviously, the pure nonlocal phase is attained by $\xi_1=0,\ \xi_2=1$, and $\xi_1=1,\ \xi_2=0$ recovers the local part participation. A hybrid part can also be obtained by $\xi_2=1-\xi_1\ ;\ 0<\xi_1<1$. Each of these items will be probed in the results section.

Eq. (43) can be expanded by replacing Eq. (38a),

$$\begin{aligned}t_{xx}(x)=&-\left(z\frac{q_{31}^2}{a_{33}}+C_{11}z+h_{31}\frac{q_{31}}{a_{33}}\right)\left(\xi_1\frac{d^2w(x)}{dx^2}+\frac{\xi_2}{2\tau}\int_0^{L_x}e^{-\frac{|x-s|}{\tau}}\frac{d^2w(s)}{ds^2}ds\right)\times\\&\left(C_{11}f(z)+\frac{q_{31}^2}{a_{33}}f(z)+\frac{q_{31}}{3}\left(\frac{f_{31}-h_{31}}{a_{33}}\right)\left(3f'(z)-2\right)+\frac{h_{31}q_{31}}{a_{33}}f'(z)+h_{31}\left(\frac{f_{31}-h_{31}}{a_{33}}\right)f''(z)\right)\\&\times\left(\xi_1\frac{d\phi(x)}{dx}+\frac{\xi_2}{2\tau}\int_0^{L_x}e^{-\frac{|x-s|}{\tau}}\frac{d\phi(s)}{ds}ds\right)+\frac{q_{31}\psi}{h}\left(\xi_1+\frac{\xi_2}{2\tau}\int_0^{L_x}e^{-\frac{|x-s|}{\tau}}ds\right)\end{aligned} \tag{44}$$

The nonlocal resultants can be defined below,

$$M_x=\int_s zt_{xx}ds \tag{45a}$$

$$V_x=\int_s f(z)t_{xx}ds \tag{45b}$$

And putting Eq. (44) into Eq. (45) gives,

$$M_x = -\left(I_{21}+I_{22}\right)\left(\xi_1\frac{d^2w(x)}{dx^2}+\frac{\xi_2}{2\tau}\int_0^{L_x}e^{-\frac{|x-s|}{\tau}}\frac{d^2w(s)}{ds^2}ds\right)$$
$$+\left(I_{23}+I_{24}+I_{25}+I_{2110}+I_{2111}\right)\left(\xi_1\frac{d\phi(x)}{dx}+\frac{\xi_2}{2\tau}\int_0^{L_x}e^{-\frac{|x-s|}{\tau}}\frac{d\phi(s)}{ds}ds\right) \tag{46a}$$

$$V_x = -\left(I_{23}+I_{24}+I_{2112}\right)\left(\xi_1\frac{d^2w(x)}{dx^2}+\frac{\xi_2}{2\tau}\int_0^{L_x}e^{-\frac{|x-s|}{\tau}}\frac{d^2w(s)}{ds^2}ds\right)$$
$$+\left(I_{212}+I_{213}+I_{214}+I_{2113}+I_{2114}\right)\left(\xi_1\frac{d\phi(x)}{dx}+\frac{\xi_2}{2\tau}\int_0^{L_x}e^{-\frac{|x-s|}{\tau}}\frac{d\phi(s)}{ds}ds\right)+I_{215} \tag{46b}$$

Consequently, the consistent and well-conditioning piezomagnetic nano model consisting of inverse flexomagneticity can be presented as follows,

$$-\left(I_{21}+I_{22}\right)\left[\xi_1\frac{d^4w(x)}{dx^4}+\frac{\xi_2}{2\tau}\frac{d^2}{dx^2}\left(\int_0^{L_x}e^{-\frac{|x-s|}{\tau}}\frac{d^2w(s)}{ds^2}ds\right)\right]+$$
$$\left(I_{23}+I_{24}+I_{25}+I_{2110}+I_{2111}\right)\left[\xi_1\frac{d^3\phi(x)}{dx^3}+\frac{\xi_2}{2\tau}\frac{d^2}{dx^2}\left(\int_0^{L_x}e^{-\frac{|x-s|}{\tau}}\frac{d\phi(s)}{ds}ds\right)\right] \tag{47a}$$
$$+\left(I_{28}+I_{29}+I_{210}\right)\frac{d^3\phi}{dx^3}-I_{27}\frac{d^4w}{dx^4}+N_x^0\frac{d^2w}{dx^2}=0$$

$$\left(I_{23}+I_{24}+I_{2112}\right)\left[\xi_1\frac{d^3w(x)}{dx^3}+\frac{\xi_2}{2\tau}\frac{d}{dx}\left(\int_0^{L_x}e^{-\frac{|x-s|}{\tau}}\frac{d^2w(s)}{ds^2}ds\right)\right]$$
$$-\left(I_{212}+I_{213}+I_{214}+I_{2113}+I_{2114}\right)\left[\xi_1\frac{d^2\phi(x)}{dx^2}+\frac{\xi_2}{2\tau}\frac{d}{dx}\left(\int_0^{L_x}e^{-\frac{|x-s|}{\tau}}\frac{d\phi(s)}{ds}ds\right)\right] \tag{47b}$$
$$-\left(I_{216}+I_{217}+I_{218}\right)\frac{d^2\phi}{dx^2}+\left(I_{28}+I_{2115}\right)\frac{d^3w}{dx^3}+I_{26}\phi=0$$

where

$$N_x^0 = q_{31}\frac{\psi}{h}\int_{-h/2}^{h/2} dz - N^0 \tag{48}$$

where we refused any supposition regarding nonlocal effects on the axial force. However, some researchers supposed it in the nonlocal form [30].

As seen, this new model contains reverse flexomagnetic parameter (h_{31}), together with the piezomagnetic influence. Thus, regardless of the solution process which is going to be applied, this modified FM model can deserve to present the converse flexomagneticity well.

It normally requires an arduous mathematical process to compute eigenvalues for an integral operator; then, the equivalent differential theory has been used instead. The entity of the square integrable solution ($L^2[a,b]$) invokes the first kind Fredholm integral equation, which has been transferred into the first kind of Volterra integral equations here through calibrating the integral limit. This issue basement divides the nonlocal integral into two parts as [31],

$$\int_a^b e^{-\frac{|x-s|}{\tau}}\sigma(s)ds = e^{-\frac{x}{\tau}}\int_a^x e^{\frac{s}{\tau}}\sigma(s)ds + e^{\frac{x}{\tau}}\int_x^b e^{-\frac{s}{\tau}}\sigma(s)ds \tag{49}$$

Then, implying the above-mentioned relation on the Eq. (47) provides a desirable solution.

2.3.2 Nonlocal differential model

In this subsection, the integral-type of the nonlocal model will be shifted to its nonlocal differential equivalent. Broad attention has been received from researchers for the nonlocal differential model to study the mechanics of nanoparticles [42-66]. This model has extended the main concept of classical mechanics, and it makes a possibility to predict the mechanical response of nanostructures more or less. Hence, this model has been further popular for the sake

of straightforwardly and facility. However, it is merely an approximate for the integral-type and incorporates a weak nonlocality. In the following, the nonlocal stress-strain elasticity relation is expressed,

$$\left(1-\tau^2\frac{d^2}{dx^2}\right)\sigma_{xx}=C_{11}\varepsilon_{xx} \tag{50}$$

Next, let re-establish the stress and higher-order stress resultants as,

$$M_x=\int_{-h/2}^{h/2}\sigma_{xx}zdz \tag{51}$$

$$V_x=\int_{-h/2}^{h/2}\sigma_{xx}f\left(z\right)dz \tag{52}$$

Following the procedure, one allows extending the resultants mentioned above as follows,

$$M_{xx}=\tau^2\frac{d^2M_x}{dx^2}-\left(I_{21}+I_{22}\right)\frac{d^2w}{dx^2}+\left(I_{23}+I_{24}+I_{25}+I_{2110}+I_{2111}\right)\frac{d\phi}{dx} \tag{53a}$$

$$V_x=\tau^2\frac{d^2V_x}{dx^2}-\left(I_{23}+I_{24}+I_{2112}\right)\frac{d^2w}{dx^2}+\left(I_{212}+I_{213}+I_{214}+I_{2113}+I_{2114}\right)\frac{d\phi}{dx}+I_{215} \tag{53b}$$

Let us re-write Eq. (29) and re-organize them on the basis of Eq. (53),

$$\frac{d^2M_x}{dx^2}=-\frac{d^2T_{xxz}}{dx^2}-N_x^0\frac{d^2w}{dx^2} \tag{54a}$$

$$\frac{d^2V_x}{dx^2}=\frac{dQ_x}{dx}-\frac{d^2R_x}{dx^2} \tag{54b}$$

Then, Eq. (54) enables to simplify Eq. (53) as,

$$M_x = -\tau^2\left(-I_{27}\frac{d^4w}{dx^4}+\left(I_{28}+I_{29}+I_{210}\right)\frac{d^3\phi}{dx^3}+N_x^0\frac{d^2w}{dx^2}\right)-\left(I_{21}+I_{22}\right)\frac{d^2w}{dx^2} \\ +\left(I_{23}+I_{24}+I_{25}+I_{2110}+I_{2111}\right)\frac{d\phi}{dx} \tag{55a}$$

$$V_x = \tau^2\left(I_{26}\frac{d\phi}{dx}+\left(I_{28}+I_{2115}\right)\frac{d^4w}{dx^4}-\left(I_{216}+I_{217}+I_{218}\right)\frac{d^3\phi}{dx^3}\right) \\ -\left(I_{23}+I_{24}+I_{2112}\right)\frac{d^2w}{dx^2}+\left(I_{212}+I_{213}+I_{214}+I_{2113}+I_{2114}\right)\frac{d\phi}{dx}+I_{215} \tag{55b}$$

It is now possible to supply differential-type nonlocal stability equation for the PFM nano scaled beam as,

$$\tau^2 I_{27}\frac{d^6w}{dx^6}-\left(\tau^2 N_x^0+I_{21}+I_{22}+I_{27}\right)\frac{d^4w}{dx^4}+N_x^0\frac{d^2w}{dx^2}-\tau^2\left(I_{28}+I_{29}+I_{210}\right)\frac{d^5\phi}{dx^5} \\ +\left(I_{23}+I_{24}+I_{25}+I_{28}+I_{29}+I_{210}+I_{2110}+I_{2111}\right)\frac{d^3\phi}{dx^3}=0 \tag{56a}$$

$$-\tau^2\left(I_{28}+I_{2115}\right)\frac{d^5w}{dx^5}+\left(I_{23}+I_{24}+I_{28}+I_{2112}+I_{2115}\right)\frac{d^3w}{dx^3} \\ -\left(\tau^2 I_{26}+I_{212}+I_{213}+I_{214}+I_{216}+I_{217}+I_{218}+I_{2113}+I_{2114}\right)\frac{d^2\phi}{dx^2} \\ +\tau^2\left(I_{216}+I_{217}+I_{218}\right)\frac{d^4\phi}{dx^4}+I_{26}\phi=0 \tag{56b}$$

The presence of reverse FM is obviously indicated by way of h_{31} in the above equations.

3 Solution strategy

The way to look for numerical examples for integral model (Eq. (47)) and differential one (Eq. (56)) is here undertaken with an analytical method. According to the results conducted by [31], the boundary condition is a potent element to illustrate disagreements between differential and integral models of nonlocality. Thus, we establish numerical results for simply-supported (S) and Clamped (C) end constraints pursuing the conditions coming along below,

- Simply-supported (S): $w=\phi=M_x=0$ at x=0, L_x

- Clamped (C): $w=\phi=0$ at x=0, L_x

Having satisfied with the corresponding permissible expression well-used earlier [67, 68],

$$w(x)=\sum_{m=1}^{\infty}W_m X_m(x) \tag{57a}$$

$$\phi(x)=\sum_{m=1}^{\infty}\Phi_m X'_m(x) \tag{57b}$$

in which the differentiation with reference to x is denoted with $(\ )'$. And,

$$X_m(x)=K_1\sin(\lambda_m x)+K_2\sinh(\lambda_m x)-\Lambda_m\left(K_3\cos(\lambda_m x)+K_4\cosh(\lambda_m x)\right) \tag{58}$$

Also, W_m and Ψ_m describe unknown Fourier coefficients mathematically. Coefficients K_i are apparently shown in detail by assisting Table 1.

Table 1

Definition of variables appeared in Eq. (58) concerning various boundary conditions (BCs).

BCs	K_i	λ_m	Λ_m
S-S	$K_1=1,\ K_2=0,$ $K_3=0,\ K_4=0$	$m\pi/L_x$	1
C-S	$K_1=1,\ K_2=-1,$ $K_3=1,\ K_4=-1$	$\tan\lambda_m=\tanh\lambda_m$	$\dfrac{\sin(\lambda_m L_x)+\sinh(\lambda_m L_x)}{\cos(\lambda_m L_x)+\cosh(\lambda_m L_x)}$
C-C	$K_1=1,\ K_2=-1,$ $K_3=1,\ K_4=-1$	$\cos\lambda_m\cosh\lambda_m=-1$	$\dfrac{\sin(\lambda_m L_x)-\sinh(\lambda_m L_x)}{\cos(\lambda_m L_x)-\cosh(\lambda_m L_x)}$

Inserting Eq. (57) into Eq. (56) leads to

$$\tau^2 I_{27}\alpha_6 W_m - \left(\tau^2 N_x^0 + I_{27} + I_{21} + I_{22}\right)\alpha_4 W_m + N_x^0 \alpha_2 W_m - \tau^2\left(I_{28} + I_{29} + I_{210}\right)\beta_5 \Phi_m$$
$$+\left(I_{23} + I_{24} + I_{25} + I_{28} + I_{29} + I_{210} + I_{2110} + I_{2111}\right)\beta_3 \Phi_m = 0 \tag{59a}$$

$$-\tau^2\left(I_{28} + I_{2115}\right)\alpha_5 W_m + \left(I_{23} + I_{24} + I_{28} + I_{2112} + I_{2115}\right)\alpha_3 W_m$$
$$-\left(\tau^2 I_{26} + I_{212} + I_{213} + I_{214} + I_{216} + I_{217} + I_{218} + I_{2113} + I_{2114}\right)\beta_2 \Phi_m \tag{59b}$$
$$+\tau^2\left(I_{216} + I_{217} + I_{218}\right)\beta_4 \Phi_m + I_{26}\beta_1 \Phi_m = 0$$

where the variables α_i and β_i can be seen in Appendix C. Then,

$$\begin{bmatrix} \begin{bmatrix} -\begin{pmatrix} \tau^2 N_x^0 + I_{27} \\ +I_{21} + I_{22} \end{pmatrix}\alpha_4 \\ +N_x^0\alpha_2 + \tau^2 I_{27}\alpha_6 \end{bmatrix} & \begin{bmatrix} \begin{pmatrix} I_{23} + I_{24} + I_{25} \\ +I_{28} + I_{29} + I_{210} \\ +I_{2110} + I_{2111} \end{pmatrix}\beta_3 \\ -\tau^2\begin{pmatrix} I_{28} + I_{29} \\ +I_{210} \end{pmatrix}\beta_5 \end{bmatrix} \\ \begin{bmatrix} \begin{pmatrix} I_{23} + I_{24} \\ +I_{28} \\ +I_{2112} + I_{2115} \end{pmatrix}\alpha_3 \\ -\tau^2\left(I_{28} + I_{2115}\right)\alpha_5 \end{bmatrix} & \begin{bmatrix} \tau^2\left(I_{216} + I_{217} + I_{218}\right)\beta_4 \\ +I_{26}\beta_1 - \begin{pmatrix} \tau^2 I_{26} + I_{212} + I_{213} \\ +I_{214} + I_{216} + I_{217} \\ +I_{218} + I_{2113} + I_{2114} \end{pmatrix}\beta_2 \end{bmatrix} \end{bmatrix} \begin{Bmatrix} W_m \\ \Phi_m \end{Bmatrix} = 0 \tag{60}$$

where determinant of coefficients computes bifurcation buckling loads.

4 Results comparison

Let us compare our beam model solution technique with some reliable references. To function with this, the results of [43, 69-71] have been carried out tabulating Tables 2-4. The data in Table 2 have been collected on account of the different BCs from ref [69]. Accordingly, the results of this reference for the C-C and C-S conditions are a little different from those of ours. The reason may be in different beam models and solution processes. However, going to Table 3 which has been added by additional references [70, 71] to complete this validation path, displays a good agreement for the aforesaid BCs. In addition, comparison in Table 4 has been

performed for higher-order beam theories, and this table can more appropriately corroborate the present results in light of the fact that the present results have been calculated for a higher-order beam model. The agreements in all the shown tables permit the extraction of the principal results and discussions.

Table 2. Dimensionless critical buckling load ($\overline{N} = NL^2/C_{11}I$, L_x/h=10, C_{11}=30e6, υ=0.3, h=varied)

τ^2	[69]			Present NDM		
	S-S	C-S	C-C	S-S	C-S	C-C
0	9.86960	20.19073	39.47842	9.62275	19.5968	36.5449
0.000025	9.86958	20.17045	39.43858	9.62273	19.5967	36.5445
0.0025	9.8672	19.9804	39.0485	9.62044	19.5872	36.5115
0.25	9.6319	17.5368	32.9505	9.39669	18.6815	33.4852
0.5	9.4055	16.2445	29.5604	9.18101	17.8479	30.8984
1	8.9830	14.4205	24.9354	8.77805	16.3856	26.7633
2	8.2426	12.0418	19.3589	8.06969	14.0787	21.1126
3	7.6149	10.4517	15.9592	7.46711	12.3412	17.4321
4	7.0761	9.2784	13.6240	6.94827	10.9854	14.8444
5	6.6085	8.3647	11.9070	6.49685	9.89807	12.9256

Table 3. Dimensionless critical buckling load ($\overline{N} = NL^2/C_{11}I$, L_x/h=10, C_{11}=30e6, υ=0.3, h=varied)

τ^2	C-S		C-C		
	Present NDM	[70]	Present NDM	[70]	[71]
0	19.5968	20.1997	36.5449	39.4786	39.4781
0.25	18.6815	19.2206	33.4852	35.9320	35.1000
1	16.3856	16.7988	26.7633	28.3044	30.3811
4	10.9854	11.1699	14.8444	15.3068	-

Table 4. Dimensionless critical buckling load ($\overline{N} = NL^2/C_{11}I$, L_x/h=10, C_{11}=30e6, υ=0.3, h=varied)

τ^2	[43]			Present
	S-S			NDM
	TBT	RBT	LBT	S-S
0	9.6227	9.6228	9.6630	9.6228
0.5	9.1701	9.1702	9.2085	9.1810
1	8.7583	8.7583	8.7949	8.7780
2	8.0364	8.0364	8.0700	8.0696
3	7.4244	7.4245	7.4555	7.4671
4	6.8990	6.8991	6.9279	6.9482
5	6.4431	6.4432	6.4701	6.4968

5 Results presentation

Let us commence the results argues by assuming that $h_{ijkl} = -f_{ijkl}$ and ignoring the direct FM parameter in Eqs. (47) and (56). Moreover, materials properties for the utilized piezomagnetic structure are tabulated by dint of Table 5 [9-23]. Finally, it is germane to note that all the numerical results have been given for the first buckling mode.

Table 5. Properties of the piezomagnetic ceramic nanobeam

$CoFe_2O_4$
C_{11}=286 GPa, v=0.32
f_{31}=10^{-9} N/A
q_{31}=580.3 N/A.m
a_{33}=1.57×10^{-4} N/A^2

We here abbreviate the nonlocal integral and differential models with NIM and NDM, respectively. First, with the help of Figures 2a-2d, we examine the difference between the results of the assumed beam-like structure in the forms of piezomagnetic-flexomagnetic (PFM), piezomagnetic with the removal of flexomagnetic effect (PM), and simple beam without any

magnetic effect (NB). Figures 2a and 2b are prepared for the boundary condition of two hinge edges, and Figures 2c and 2d are provided for the boundary condition of two fixed ends. In Figures 2a and 2c, the local phase of the integral model is ignored, and the nonlocal phase is investigated only. A superficial look at all figures shows that the NIM, like the NDM, leads to the softness of the material, and here the critical buckling load is reduced by increasing the nonlocal parameter. However, the reduction slope of the results is observed differently for both integral and differential models. It should be cognizant that to find the results for τ=0 (locality), the integral model is implemented in the local phase mode. This is true in the rest and the whole results of the article. In addition, here, it is also specified analogously to the literature that the PFM beam is more rigid than the PM beam and the NB one, respectively. This means that the flexomagnetic impact leads to the greater rigidity of the material, which has been proven in all literature. What is more, the figures demonstrate that the nonlocal sensitivity of the pure NIM is more than NDM by a change in the nonlocal coefficient. A deeper look at the figures proves that in PFM beam analysis, the difference between the integral and differential models results is reduced, and the largest difference is seen in the NB beam. Thus, it can be argued that the FM effect will reduce the importance of using the integral model.

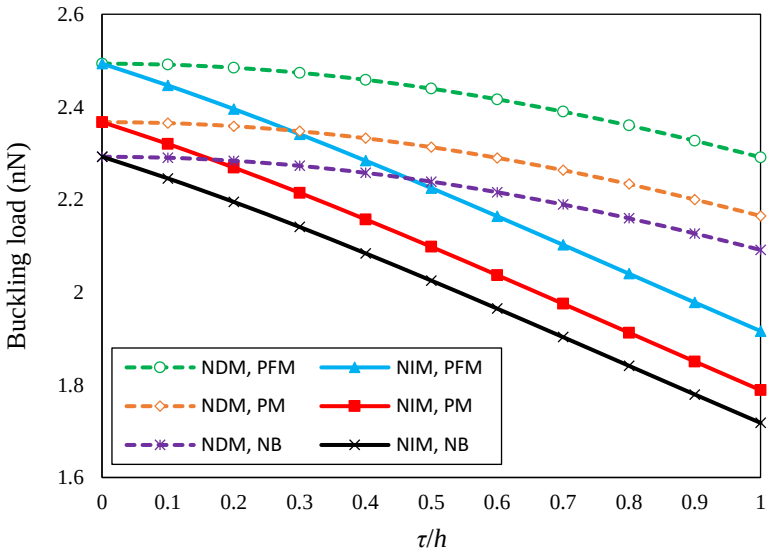

Figure 2a. Nonlocal parameter vs. buckling load for different small scale beams and assigned conditions including ψ=1e-4A, L_x=10h, l=0.05h, ξ_1=0, ξ_2=1, S-S.

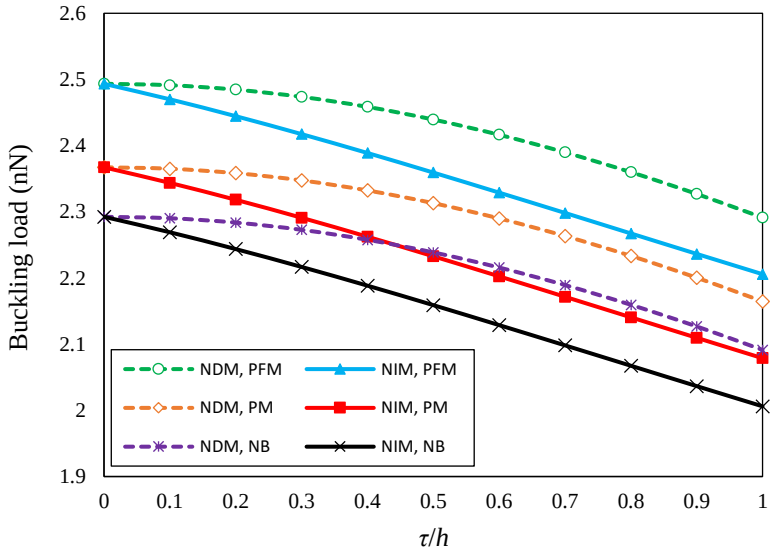

Figure 2b. Nonlocal parameter vs. buckling load for different small scale beams and assigned conditions including ψ=1e-4A, L_x=10h, l=0.05h, ξ_1=0.5, ξ_2=0.5, S-S.

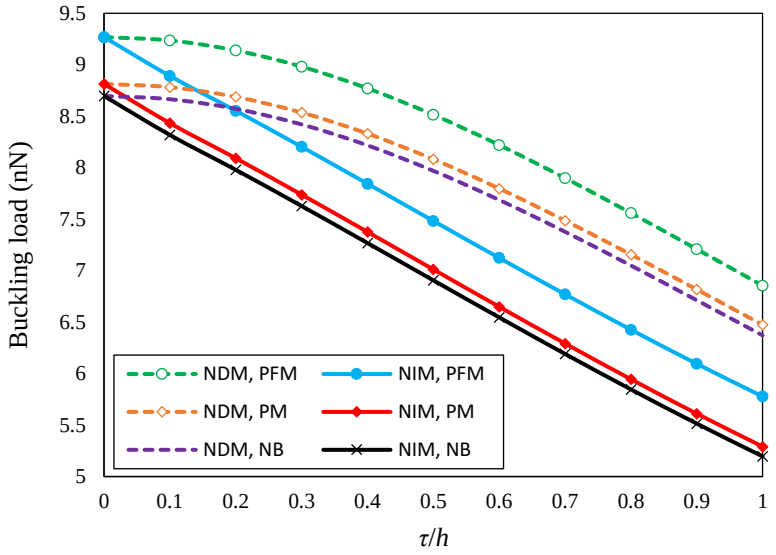

Figure 2c. Nonlocal parameter vs. buckling load for different small scale beams and assigned conditions including ψ=1e-4A, L_x=10h, l=0.05h, ξ_1=0, ξ_2=1, C-C.

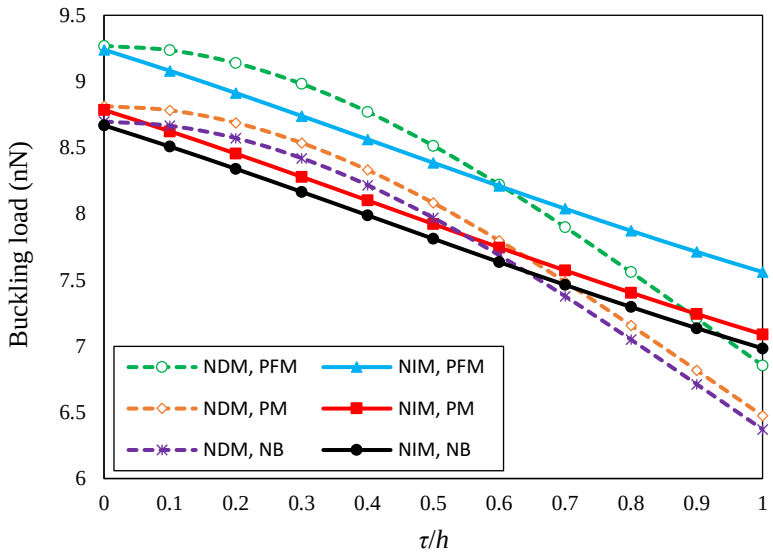

Figure 2d. Nonlocal parameter vs. buckling load for different small scale beams and assigned conditions including ψ=1e-4A, L_x=10h, l=0.05h, ξ_1=0.5, ξ_2=0.5, C-C.

In the following, by drawing Figures 3a and 3b, the results in a variety of boundary conditions and in both nonlocal models with changes in the amount of the nonlocal coefficient have been examined. Figure 3a has been presented for the integral model based on single-phase nonlocality, and Figure 3b has been illustrated for the hybrid phase of the integral model. As it is evident, the larger value of the nonlocal parameter increases the difference between the NIM and NDM. This difference in the first figure is much greater for the non-hybrid phase. Interestingly, with the increase of the nonlocal parameter, in the differential model, the results for different boundary conditions will be closer to each other with a larger inclination, and this tendency is less inclined in the integral model. This finding can be unrelated to the result of the previous figures, which we obtained the pure NIM is more sensitive to the nonlocal coefficient. It means that when using a hybrid NIM, the NIM is less sensitive to the nonlocal parameter. On the other hand, with the assistance of Figure 3b, it can be concluded that the clamped boundary condition will make the greatest difference between the two nonlocal models. It goes without saying that the results of these two figures are obtained for the PFM beam.

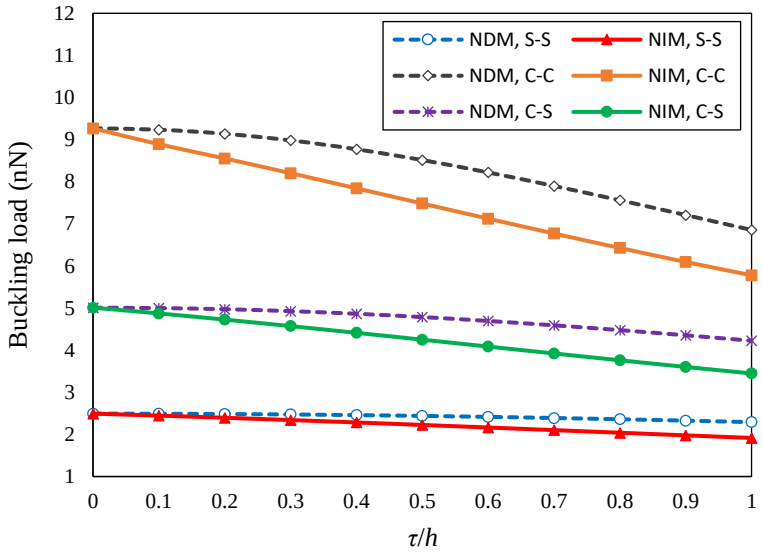

Figure 3a. Nonlocal parameter vs. buckling load for different BCs and assigned conditions including ψ=1e-4A, L_x=10h, l=0.05h, ξ_1=0, ξ_2=1.

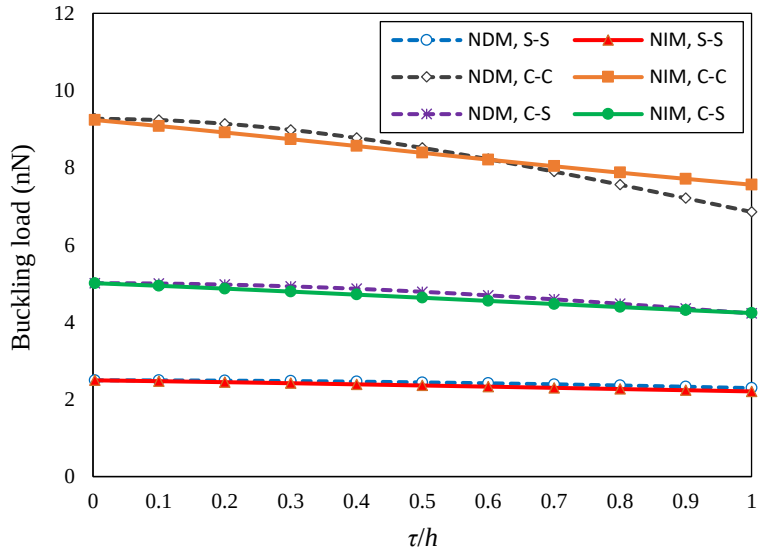

Figure 3b. Nonlocal parameter vs. buckling load for different BCs and assigned conditions including ψ=1e-4A, L_x=10h, l=0.05h, ξ_1=0.5, ξ_2=0.5.

Strain gradient parameter variations can also be analyzed to evaluate the results better. For this purpose, Figures 4a-4d are plotted, which show the results for different boundary conditions. The first two figures are for the single-phase nonlocal integral model where the local phase is left out for the NIM (pure nonlocal case), and the second two figures are displayed

for the hybrid phase. It is quite vivid that the coincidence of results of the NDM to those of the NIM depends on boundary conditions. For S-S, the NDM results are nearer to those of the hybrid NIM's. For other boundary conditions, it seems that the NDM results are far from those of the NIM. Although the basis for having higher accuracy and efficiency is the integral model (the nonlocal differential model is only an approximation for the NIM), the hybrid phase may present steady higher results values compared to NDM, and this bigness is higher in results of boundary conditions with lower degrees of freedom. According to the results, the differential model is a reasonable estimation of the integral model in the case where the amounts of the nonlocal parameter are very little. It is to be noted that when l/h=0, in fact, the PM structure comes along due to the very small amount of FM parameter. Whatever the value of SGLS is considerable, the FM effect is more indispensable.

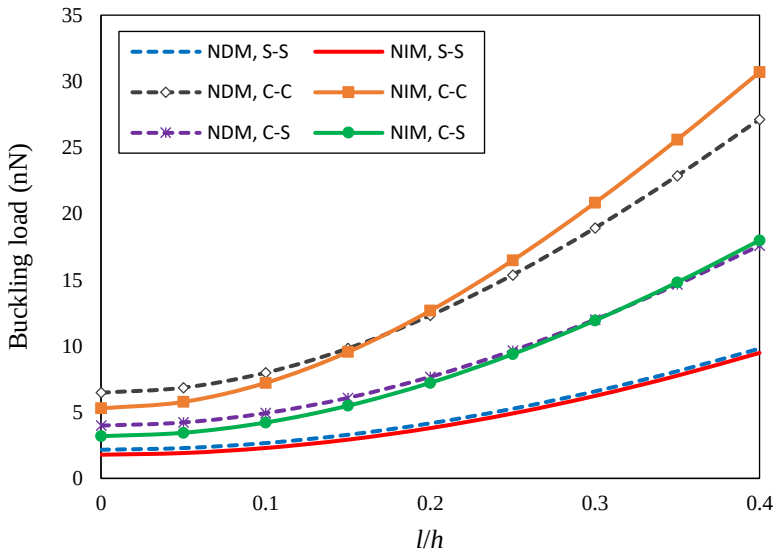

Figure 4a. SGLS parameter vs. buckling load for different BCs and assigned conditions including ψ=1e-4A, L_x=10h, τ=h, ξ_1=0, ξ_2=1.

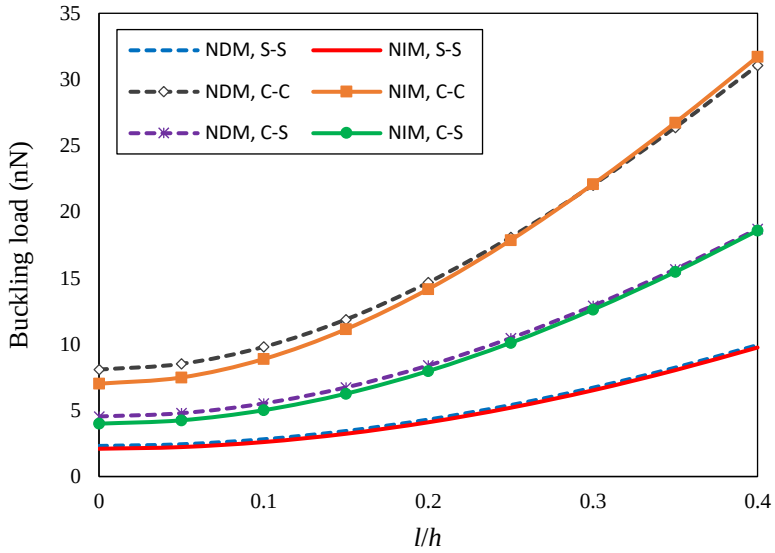

Figure 4b. SGLS parameter vs. buckling load for different BCs and assigned conditions including ψ=1e-4A, L_x=10h, τ=0.5h, ξ_1=0, ξ_2=1.

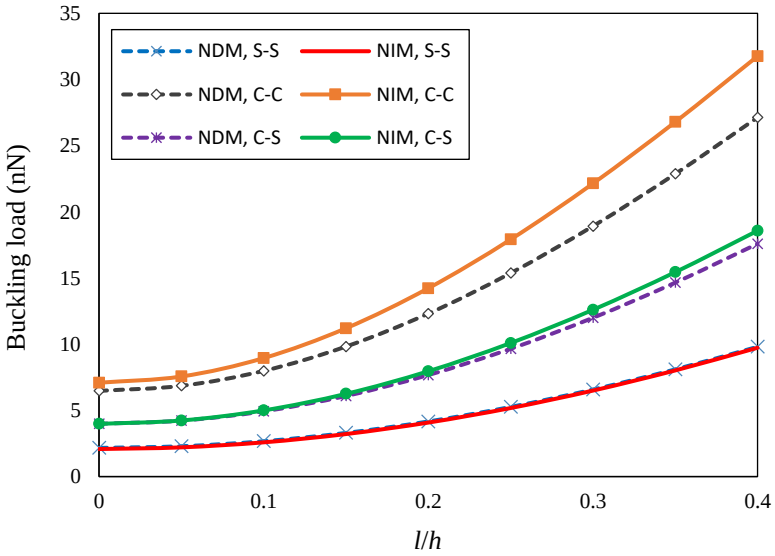

Figure 4c. SGLS parameter vs. buckling load for different BCs and assigned conditions including ψ=1e-4A, L_x=10h, τ=h, ξ_1=0.5, ξ_2=0.5.

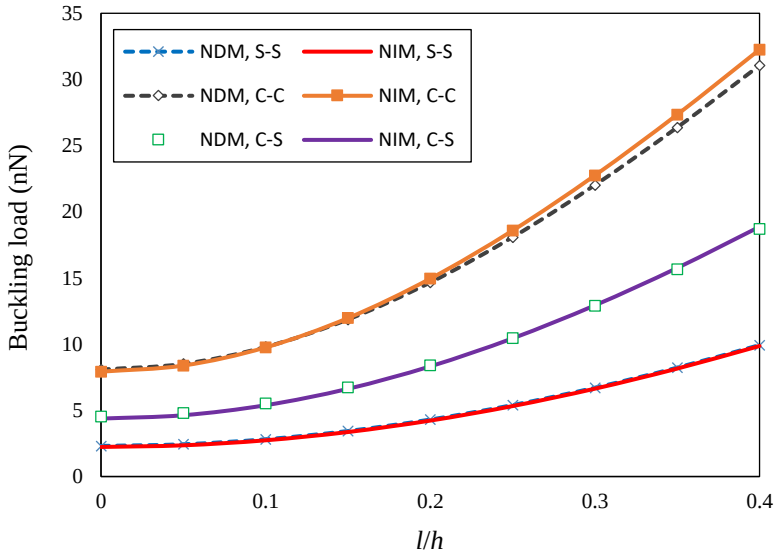

Figure 4d. SGLS parameter vs. buckling load for different BCs and assigned conditions including ψ=1e-4A, L_x=10h, τ=0.5h, ξ_1=0.5, ξ_2=0.5.

Now, the attention has been turned to Figures 5a-5d, in which the changes in the ratio of length to thickness have been studied. Again, all conditions and variables are applied as in the previous figures. The first two figures show that increasing the beam's length will reduce the difference in results of all boundary conditions for both nonlocal integral and differential models. The shift between the results of the integral model and the differential type again shows more sense in using the NIM. The most important extractive result of this section can be that for thicker beams, the difference between the results of the two nonlocal models will increase. It implies that the importance of using the NIM for thicker beams increases. In contrast, the NDM is well-conjecture for the NIM when the beam is thinner.

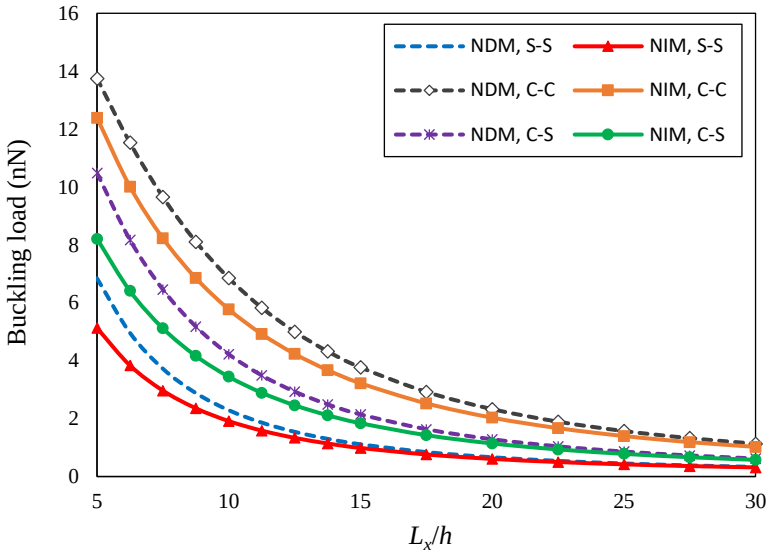

Figure 5a. Slenderness ratio vs. buckling load for different BCs and assigned conditions including ψ=1e-4A, l=0.05h, τ=h, ξ_1=0, ξ_2=1.

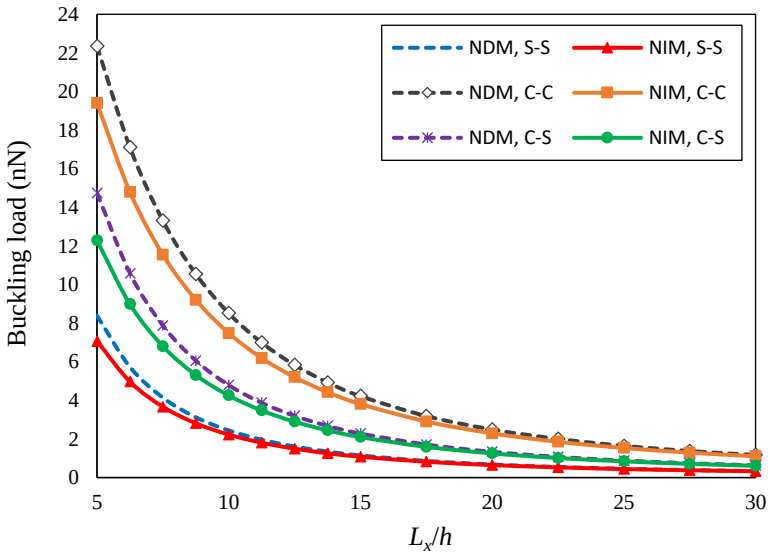

Figure 5b. Slenderness ratio vs. buckling load for different BCs and assigned conditions including ψ=1e-4A, l=0.05h, τ=0.5h, ξ_1=0, ξ_2=1.

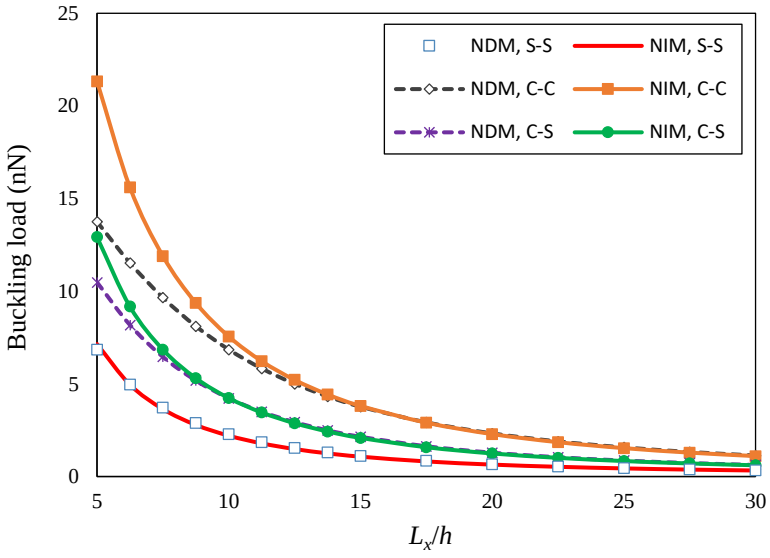

Figure 5c. Slenderness ratio vs. buckling load for different BCs and assigned conditions including ψ=1e-4A, l=0.05h, τ=h, ξ_1=0.5, ξ_2=0.5.

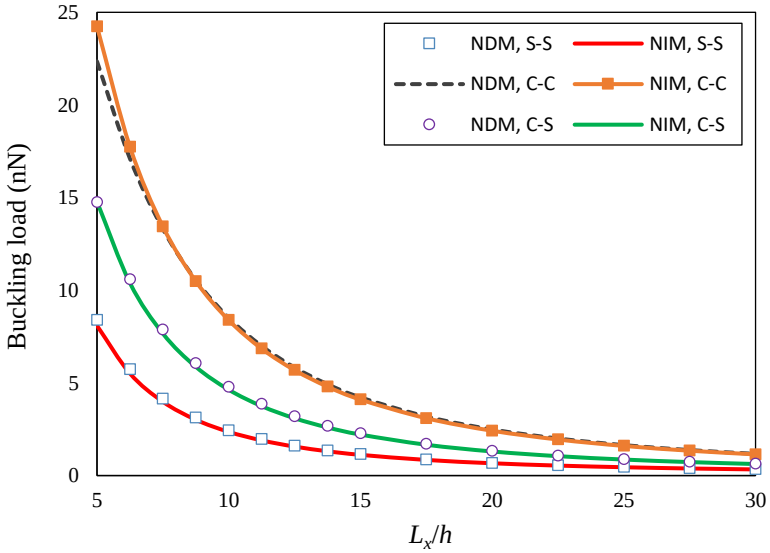

Figure 5d. Slenderness ratio vs. buckling load for different BCs and assigned conditions including ψ=1e-4A, l=0.05h, τ=0.5h, ξ_1=0.5, ξ_2=0.5.

Figures 6a-6d provide a brief overview of the impact of magnetic potential changes. The increase in the external magnetic potential in both figures appears to be almost linear. In fact, this magnetic potential is derived from the external magnetic field, which is applied to the topmost and bottommost outer surfaces of the beam in the direction of thickness, which in turn is a short field. Due to the gradient of axial strain, this external magnetic field causes

magnetization in the beam laterally, which eventually causes deformation. This is exactly the converse flexoeffect. This magnetization and the production of an internal magnetic field lead to creating a force perpendicular to the field. Since the field is created in the direction of thickness, so the established force is along with the longitudinal axis, which as a result, it compresses and contracts the beam. This is why the greater the magnetic potential, the higher the critical buckling load. When the material is denser, in fact, its stiffness has increased, and more mechanical force is needed for the beam to reach the buckle and bifurcation. Reviewing the figures, it is delineated that the NDM results have an orientation to those of the hybrid NIM. And documented to the pure NIM, the NDM results are mostly unacceptable unless the more flexible edge conditions are thought-out.

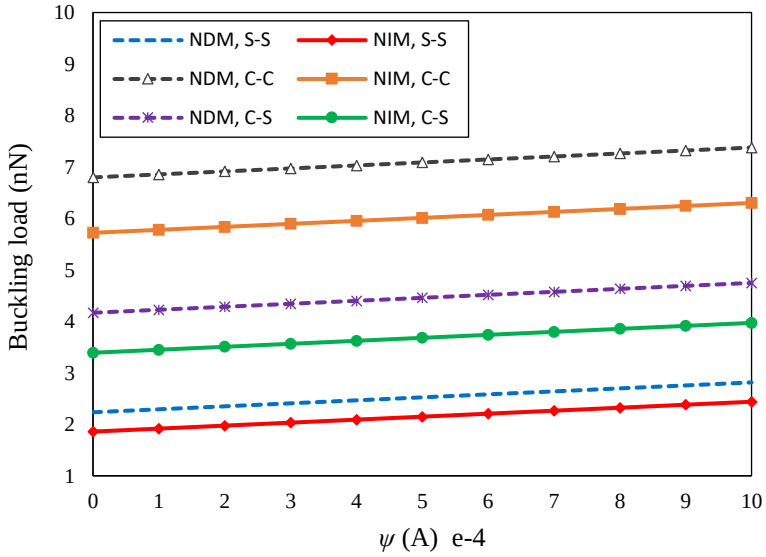

Figure 6a. Magnetic potential vs. buckling load for different BCs and assigned conditions including l=0.05h, L_x=10h, τ=h, ξ_1=0, ξ_2=1.

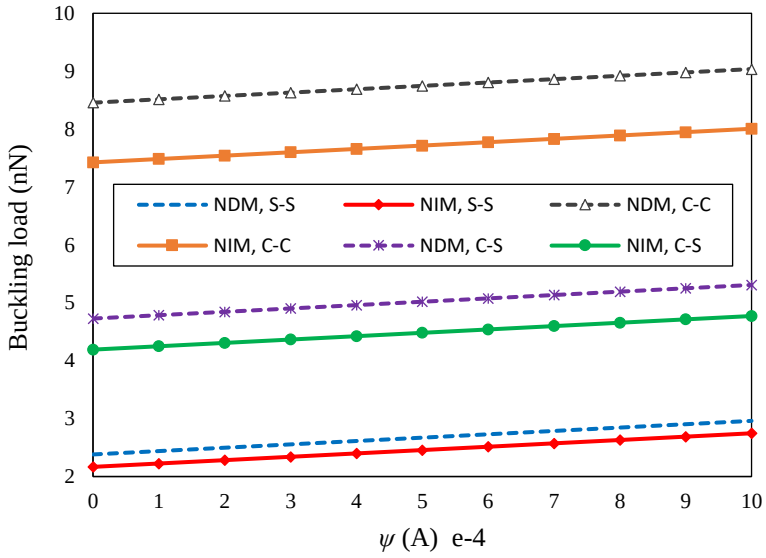

Figure 6b. Magnetic potential vs. buckling load for different BCs and assigned conditions including l=0.05h, L_x=10h, τ=0.5h, ξ_1=0, ξ_2=1.

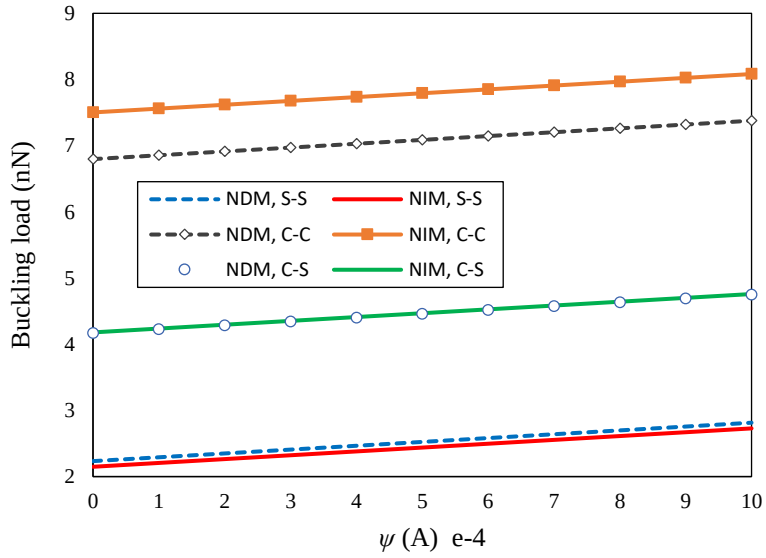

Figure 6c. Magnetic potential vs. buckling load for different BCs and assigned conditions including l=0.05h, L_x=10h, τ=h, ξ_1=0.5, ξ_2=0.5.

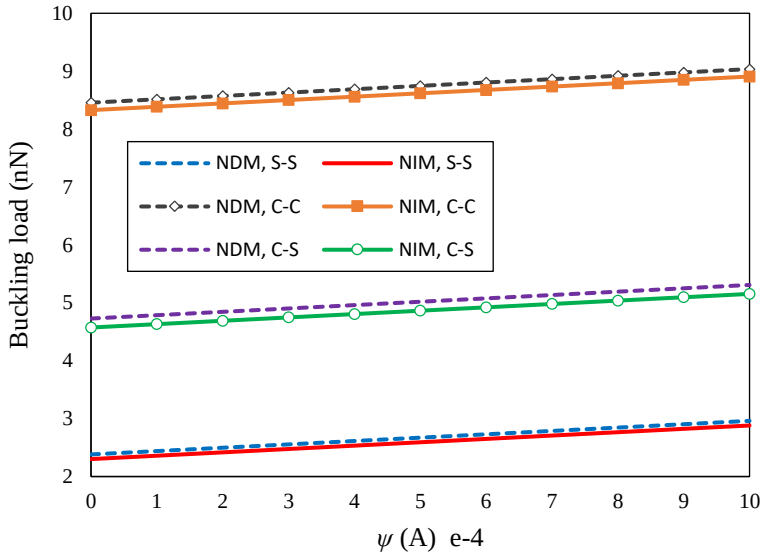

Figure 6d. Magnetic potential vs. buckling load for different BCs and assigned conditions including l=0.05h, L_x=10h, τ=0.5h, ξ_1=0.5, ξ_2=0.5.

The last figures in the results section, Figures 7a-7d are allocated to investigate the behavior of the weight factors in NIM. As observed, ξ_1 has an opposite response to ξ_2. As found out, ξ_1 has a stiffness-hardening effect, and ξ_2 makes a stiffness-softening effect into the material. Thus, while using a hybrid case of NIM, the values of both factors can play a momentous role in distinguishing the mechanical response.

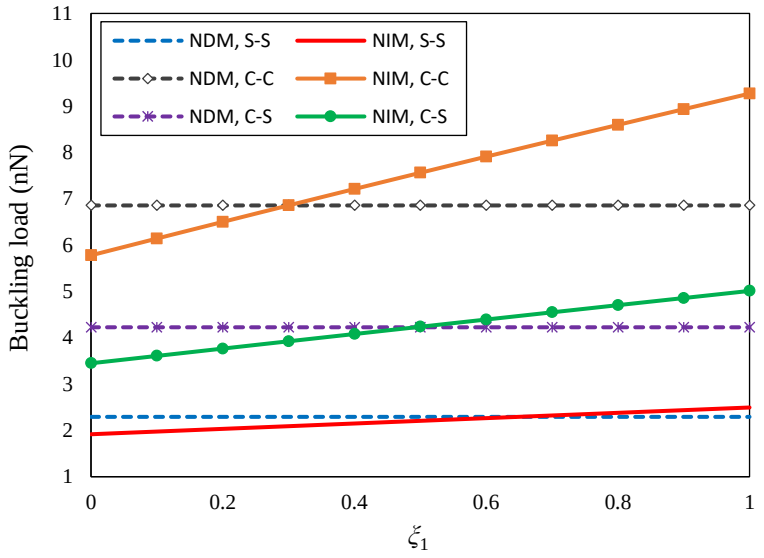

Figure 7a. First weight factor vs. buckling load for different BCs and assigned conditions including ψ=1e-4A, L_x=10h, l=0.05h, τ=h.

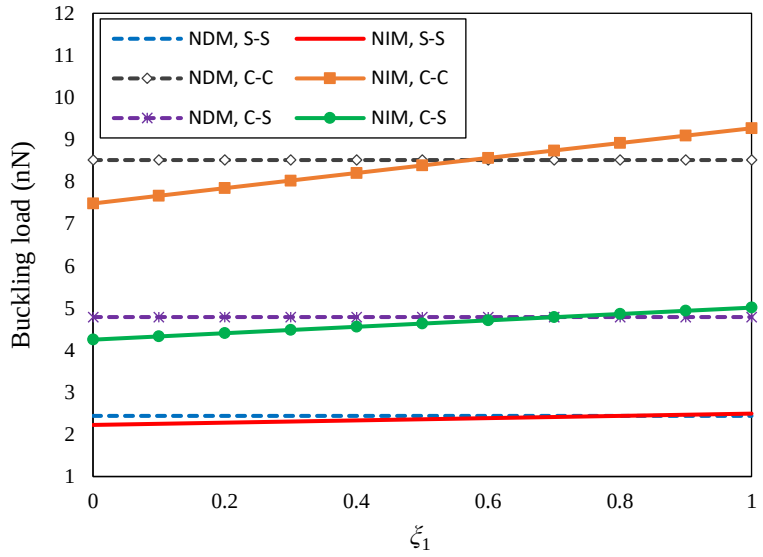

Figure 7b. First weight factor vs. buckling load for different BCs and assigned conditions including ψ=1e-4A, L_x=10h, l=0.05h, τ=0.5h.

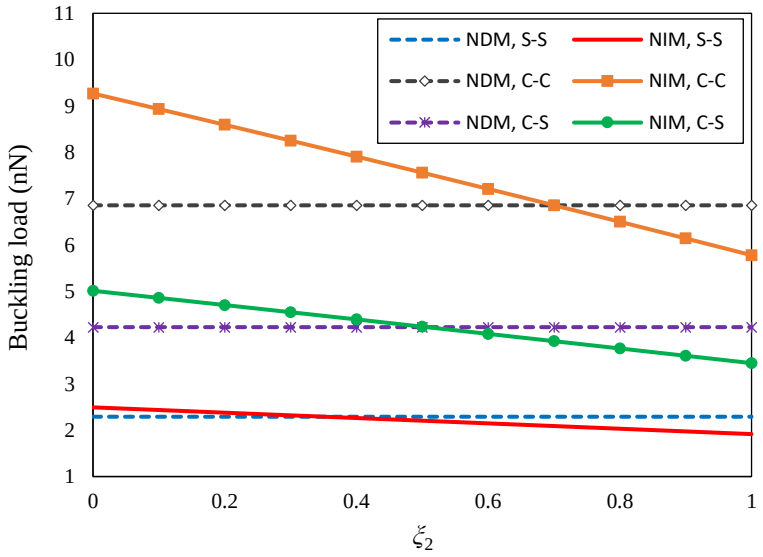

Figure 7c. Second weight factor vs. buckling load for different BCs and assigned conditions including ψ=1e-4A, L_x=10h, l=0.05h, τ=h.

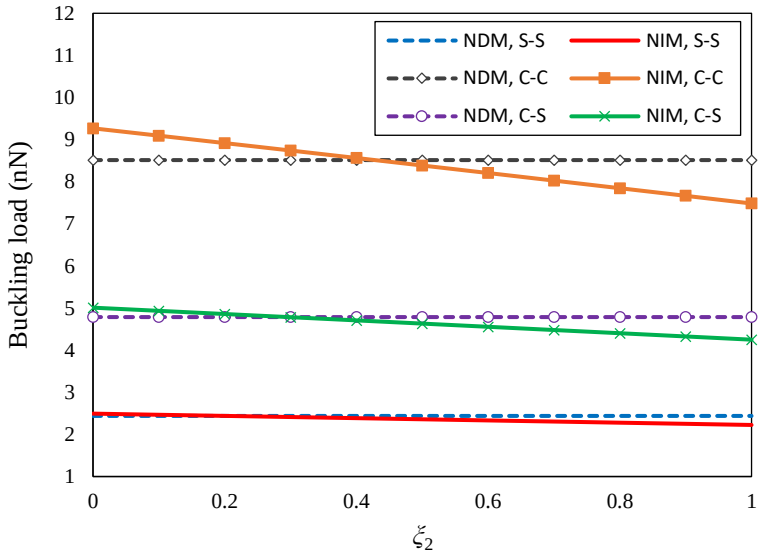

Figure 7d. Second weight factor vs. buckling load for different BCs and assigned conditions including ψ=1e-4A, L_x=10h, l=0.05h, τ=0.5h.

A series of tabulated results are organized in the following by fixing Tables 6-11 to make a benchmark section for the subsequent studies on PFM models. The assigned quantities are clearly placed beside the titles of the tables.

Table 6. SGLS parameter vs. nonlocal factor for buckling loads (nN) at S-S end conditions (L_x=10h, ψ=1e-4A, ξ_1=0, ξ_2=1, S-S)

l/h	τ=0.01h		τ=0.1h		τ=0.5h	
	NDM	NIM	NDM	NIM	NDM	NIM
0.00	2.3673	2.3628	2.3651	2.3201	2.3131	2.0980
0.05	2.4935	2.4890	2.4913	2.4464	2.4394	2.2248
0.10	2.8706	2.8661	2.8684	2.8239	2.8169	2.6038
0.15	3.4942	3.4898	3.4921	3.4481	3.4412	3.2306
0.20	4.3573	4.3530	4.3552	4.3119	4.3051	4.0979
0.25	5.4502	5.4459	5.4481	5.4057	5.3990	5.1962
0.30	6.7610	6.7569	6.7590	6.7177	6.7112	6.5133
0.35	8.2762	8.2722	8.2743	8.2341	8.2278	8.0357
0.40	9.9807	9.9769	9.9788	9.9400	9.9339	9.7481
0.45	11.8586	11.8549	11.8568	11.8194	11.8135	11.6345
0.50	13.8933	13.8897	13.8915	13.8556	13.8499	13.6781

Table 7. SGLS parameter vs. nonlocal factor for buckling loads (nN) at C-C end conditions (L_x=10h, ψ=1e-4A, ξ_1=0, ξ_2=1, C-C)

l/h	τ=0.01h		τ=0.1h		τ=0.5h	
	NDM	NIM	NDM	NIM	NDM	NIM
0.00	8.8138	8.7246	8.7823	8.4329	8.0824	7.0122
0.05	9.2687	9.1804	9.2362	8.8913	8.5145	7.4834
0.10	10.6143	10.5283	10.5789	10.2468	9.7934	8.8764
0.15	12.7949	12.7126	12.7551	12.4432	11.8690	11.1320
0.20	15.7259	15.6485	15.6803	15.3946	14.6642	14.1599
0.25	19.3031	19.2313	19.2508	18.9955	18.0841	17.8498
0.30	23.4136	23.3479	23.3541	23.1317	22.0244	22.0822
0.35	27.9456	27.8861	27.8786	27.6901	26.3808	26.7392
0.40	32.7957	32.7424	32.7214	32.5663	31.0557	31.7128
0.45	37.8743	37.8270	37.7927	37.6699	35.9632	36.9094
0.50	43.1077	43.0659	43.0191	42.9266	41.0314	42.2530

Table 8. Nonlocal parameter vs. weight factors for buckling loads (nN) at S-S end conditions (L_x=10h, l=0.05h, ψ=1e-4A, S-S)

τ/h	NDM	NIM ξ_1=1, ξ_2=0	NIM ξ_1=0.75, ξ_2=0.25	NIM ξ_1=0.5, ξ_2=0.5	NIM ξ_1=0.25, ξ_2=0.75	NIM ξ_1=0, ξ_2=1
0.0025	2.4935	2.4935	2.4932	2.4929	2.4926	2.4924
0.01	2.4935	2.4935	2.4923	2.4912	2.4901	2.4890
0.05	2.4929	2.4935	2.4877	2.4820	2.4762	2.4705
0.10	2.4913	2.4935	2.4817	2.4700	2.4582	2.4464
0.20	2.4846	2.4935	2.4690	2.4445	2.4200	2.3954
0.30	2.4737	2.4935	2.4554	2.4174	2.3793	2.3411
0.40	2.4586	2.4935	2.4412	2.3889	2.3365	2.2840
0.50	2.4394	2.4935	2.4265	2.3593	2.2921	2.2248

Table 9. Nonlocal parameter vs. weight factors for buckling loads (nN) at C-C end conditions (L_x=10h, l=0.05h, ψ=1e-4A, C-C)

τ/h	NDM	NIM	NIM	NIM	NIM	NIM

		ξ_1=1, ξ_2=0	ξ_1=0.75, ξ_2=0.25	ξ_1=0.5, ξ_2=0.5	ξ_1=0.25, ξ_2=0.75	ξ_1=0, ξ_2=1
0.0025	9.2690	9.2690	9.2527	9.2364	9.2201	9.2038
0.01	9.2687	9.2690	9.2469	9.2247	9.2026	9.1804
0.05	9.2608	9.2690	9.2153	9.1616	9.1077	9.0538
0.1	9.2362	9.2690	9.1749	9.0806	8.9860	8.8913
0.2	9.1392	9.2690	9.0913	8.9129	8.7336	8.5535
0.3	8.9821	9.2690	9.0051	8.7395	8.4721	8.2030
0.4	8.7712	9.2690	8.9175	8.5630	8.2054	7.8446
0.5	8.5145	9.2690	8.8299	8.3859	7.9371	7.4834

Table 10. SGLS parameter vs. weight factors for buckling loads (nN) at S-S end conditions (L_x=10h, τ=0.05h, ψ=1e-4A, S-S)

l/*h*	NDM	NIM ξ_1=1, ξ_2=0	NIM ξ_1=0.75, ξ_2=0.25	NIM ξ_1=0.5, ξ_2=0.5	NIM ξ_1=0.25, ξ_2=0.75	NIM ξ_1=0, ξ_2=1
0.00	2.3667	2.3673	2.3615	2.3558	2.3500	2.3442
0.05	2.4929	2.4935	2.4877	2.4820	2.4762	2.4705
0.10	2.8700	2.8706	2.8649	2.8592	2.8535	2.8478
0.15	3.4937	3.4942	3.4886	3.4830	3.4773	3.4717
0.20	4.3568	4.3573	4.3518	4.3462	4.3407	4.3351
0.25	5.4497	5.4502	5.4448	5.4393	5.4339	5.4284
0.30	6.7605	6.7610	6.7557	6.7504	6.7451	6.7398
0.35	8.2757	8.2762	8.2711	8.2659	8.2608	8.2556
0.40	9.9803	9.9808	9.9758	9.9708	9.9658	9.9608
0.45	11.8582	11.8587	11.8539	11.8491	11.8443	11.8395
0.50	13.8928	13.8933	13.8887	13.8841	13.8795	13.8749

Table 11. SGLS parameter vs. weight factors for buckling loads (nN) at C-C end conditions (L_x=10h, τ=0.05h, ψ=1e-4A, C-C)

l/*h*	NDM	NIM ξ_1=1, ξ_2=0	NIM ξ_1=0.75, ξ_2=0.25	NIM ξ_1=0.5, ξ_2=0.5	NIM ξ_1=0.25, ξ_2=0.75	NIM ξ_1=0, ξ_2=1
0.00	8.8061	8.8142	8.7599	8.7057	8.6513	8.5969
0.05	9.2608	9.2690	9.2153	9.1616	9.1077	9.0538

0.10	10.6057	10.6146	10.5623	10.5100	10.4576	10.4051
0.15	12.7852	12.7953	12.7452	12.6951	12.6449	12.5947
0.20	15.7148	15.7263	15.6792	15.6319	15.5847	15.5373
0.25	19.2904	19.3036	19.2598	19.2159	19.1720	19.1281
0.30	23.3992	23.4142	23.3741	23.3338	23.2936	23.2533
0.35	27.9293	27.9463	27.9098	27.8734	27.8368	27.8003
0.40	32.7777	32.7965	32.7637	32.7310	32.6982	32.6653
0.45	37.8545	37.8752	37.8460	37.8167	37.7875	37.7582
0.50	43.0862	43.1086	43.0827	43.0568	43.0308	43.0049

6 Conclusion

In summary, this paper has been prepared to clarify and expound some unclear and incoherencies in the available flexomagnetic (FM) theoretical model. Conjointly, an attempt has been made to propose a new general FM model that is competent for both direct and converse effects of FM. In order to establish elastic strain and strain gradient, a higher-order shear deformation beam theory has been selected. The novel FM model has been transmitted into the nonlocal phase based on the weak and strong forms of nonlocal elasticity, namely differential and integral modes. The gained mathematical models have been discussed detailedly after solving through associated analytical processes, within which various conditions have been considered for both ends of the beam-like finite-size intelligent actuator. A series comparison has been provided to illustrate results divergence of differential nonlocality vis-à-vis the integral one, evaluating several boundary conditions. We expect this research paper to play the role of a benchmark reference for MEMS/NEMS researchers and indicate the concept of flexomagneticity simpler. The contributed results become listed below,

- The disordered former flexomagnetic model has been corrected by presenting a modified FM version, which deserves both inverse and direct FM effects.

- In order to study FM in both Centro- and non-centrosymmetric crystalline structures,

the non-uniform strain has to be implemented to keep the FM parameter in the final equations. Apart from this, the FM coefficient will disappear from the final governing equations based on any flexomagnetic model.

- Flexomagnetic effect and, in general, magnetic properties lessen the discrepancy of results of NIM and NDM.

- In some cases, it was manifested that there are significant differences between results obtained by the integral form of nonlocality versus the differential one.

- The most profound differences between differential and integral forms of nonlocality have been witnessed for clamped-clamped boundary conditions and the least one through simply-supported end conditions. Thus, it can be declared that the further rigid the boundary conditions, the more recommended the use of the integral model will be.

- It can be told that the increase of the SGLS coefficient results in the further significance of the nonlocal integral model. Moreover, it showed that after a certain value of SGLS, the difference in results of NIM and NDM is enormous.

- An advantage of employing NIM is obviating the approximations of NDM during applying the Eringen relation on the governing equations (Eq. 53). In fact, the NIM does not need any supposition like that in Eq. (53).

- The use of NIM becomes more serious while the structure gets thicker.

- The NDM grants correct results if the value of the nonlocal parameter is small to some degree.

- NDM results tend to those of the hybrid NIM, and based on the single-phase pure NIM, the NDM results are not always convincing.

- NIM also has a stiffness-softening effect in all states, similar to the NDM. However, a further softening behavior has been beholden by the use of NIM when the local phase is obliterated.

Funding: This research received no external funding.

Authors' contribution:

First author: Conceptualization, Methodology, Software, Validation, Formal analysis, Investigation, Resources, Data curation, Visualization, Original draft preparation.

Second author: Review and editing, Supervision, Project administration.

References

[1] N. Mawassy, H. Reda, J.-F. Ganghoffer, V. A. Eremeyev, H. Lakiss, A variational approach of homogenization of piezoelectric composites towards piezoelectric and flexoelectric effective media, International Journal of Engineering Science 158 (2021) 103410.

[2] V. A. Eremeyev, J.-F. Ganghoffer, V. Konopińska-Zmysłowska, N. S. Uglov, Flexoelectricity and apparent piezoelectricity of a pantographic micro-bar, International Journal of Engineering Science 149 (2020) 103213.

[3] A. F. Kabychenkov, F. V. Lisovskii, Flexomagnetic and flexoantiferromagnetic effects in centrosymmetric antiferromagnetic materials, Technical Physics 64 (2019) 980-983.

[4] P. Zubko, G. Catalan, A. Buckley, P. R. L. Welche, J. F. Scott, Strain-gradient-induced polarization in SrTiO3 single crystals, Physical Review Letters 99 (2007) 167601.

[5] E. A. Eliseev, A. N. Morozovska, V. V. Khist, V. Polinger, Chapter Six - Effective flexoelectric and flexomagnetic response of ferroics, Editor(s): Robert L. Stamps, Helmut Schultheiß, Solid State Physics, Academic Pre, 70 (2019) 237-289.

[6] E. A. Eliseev, M. D. Glinchuk, V. Khist, V. V. Skorokhod, R. Blinc, and A. N. Morozovska, Linear magnetoelectric coupling and ferroelectricity induced by the flexomagnetic effect in ferroics, Physical Review B 84 (2011) 174112.

[7] E. A. Eliseev, A. N. Morozovska, M. D. Glinchuk, R. Blinc, Spontaneous flexoelectric/flexomagnetic effect in nanoferroics, Physical Review B 79 (2009) 165433.

[8] P. Lukashev, R. F. Sabirianov, Flexomagnetic effect in frustrated triangular magnetic structures, Physical Review B 82 (2010) 094417.

[9] S. Sidhardh, M. C. Ray, Flexomagnetic response of nanostructures, Journal of Applied Physics 124 (2018) 244101.

[10] N. Zhang, Sh. Zheng, D. Chen, Size-dependent static bending of flexomagnetic nanobeams, Journal of Applied Physics 126 (2019) 223901.

[11] J. Sladek, V. Sladek, M. Xu, Q. Deng, A cantilever beam analysis with flexomagnetic effect, Meccanica 56 (2021) 2281–2292.

[12] M. Malikan, V.A. Eremeyev, (2020) Free Vibration of Flexomagnetic Nanostructured Tubes Based on Stress-driven Nonlocal Elasticity. In: Altenbach H., Chinchaladze N., Kienzler R., Müller W. (eds) Analysis of Shells, Plates, and Beams. Advanced Structured Materials, vol 134. Springer, Cham.

[13] M. Malikan, V. A. Eremeyev, On the geometrically nonlinear vibration of a piezo-flexomagnetic nanotube, Mathematical Methods in the Applied Sciences, 2020. https://doi.org/10.1002/mma.6758

[14] M. Malikan, V. A. Eremeyev, On Nonlinear Bending Study of a Piezo-Flexomagnetic Nanobeam Based on an Analytical-Numerical Solution, Nanomaterials 10 (2020) 1762.

[15] M. Malikan, V. A. Eremeyev, K. K. Żur, Effect of Axial Porosities on Flexomagnetic Response of In-Plane Compressed Piezomagnetic Nanobeams, Symmetry 12 (2020) 1935.

[16] M. Malikan, N. S. Uglov, V. A. Eremeyev, On instabilities and post-buckling of piezomagnetic and flexomagnetic nanostructures, International Journal of Engineering Science 157 (2020) 10339.

[17] M. Malikan, V. A. Eremeyev, Flexomagneticity in buckled shear deformable hard-magnetic soft structures, Continuum Mechanics and Thermodynamics 34 (2021) 1-16.

[18] M. Malikan, T. Wiczenbach, V. A. Eremeyev, On thermal stability of piezo-flexomagnetic microbeams considering different temperature distributions, Continuum Mechanics and Thermodynamics 33 (2021) 1281-1297.

[19] M. Malikan, V. A. Eremeyev, Flexomagnetic response of buckled piezomagnetic composite nanoplates, Composite Structures 267 (2021) 113932.

[20] M. Malikan, T. Wiczenbach, V.A. Eremeyev, Thermal buckling of functionally graded piezomagnetic micro- and nanobeams presenting the flexomagnetic effect, Continuum Mechanics and Thermodynamics (2021). https://doi.org/10.1007/s00161-021-01038-8

[21] M. Malikan, T. Wiczenbach, V. A. Eremeyev, (2022) Flexomagneticity in Functionally Graded Nanostructures. In: Altenbach H., Eremeyev V.A., Galybin A., Vasiliev A. (eds) Advanced Materials Modelling for Mechanical, Medical and Biological Applications. Advanced Structured Materials, vol 155. Springer, Cham.

[22] M. Malikan, V. A. Eremeyev, Effect of surface on the flexomagnetic response of ferroic composite nanostructures; nonlinear bending analysis, Composite Structures 271 (2021) 114179.

[23] M. Malikan, V. A. Eremeyev, (2021) On forced vibrations of piezo-flexomagnetic nano-actuator beams. In: Chakraverty S., Tornabene F., Reddy J. N. Modeling and Computation in Vibration Problems. Numerical and semi-Analytical methods, vol 1. IOP.

[24] T.-K. Nguyen, T. T.-Ph. Nguyen, Th. P. Vo, H.-T. Thai, Vibration and buckling analysis of functionally graded sandwich beams by a new higher-order shear deformation theory, Composites Part B: Engineering 76 (2015) 273-285.

[25] Sh. Dastjerdi, B. Akgöz, Ö. Civalek, M. Malikan, V. A. Eremeyev, On the non-linear dynamics of torus-shaped and cylindrical shell structures, International Journal of Engineering Science 156 (2020) 103371.

[26] Sh. Dastjerdi, B. Akgöz, Ö. Civalek, On the shell model for human eye in Glaucoma disease, International Journal of Engineering Science 158 (2021) 103414.

[27] B. Karami, M. Janghorban, H. Fahham, On the stress analysis of anisotropic curved panels, International Journal of Engineering Science 172 (2022) 103625.

[28] Sh. Zhou, A. Li, B. Wang, A reformulation of constitutive relations in the strain gradient elasticity theory for isotropic materials, International Journal of Solids and Structures 80 (2016) 28-37.

[29] A. C. Eringen, (2002) Nonlocal continuum field theories. Springer, New York.

[30] M. Faraji Oskouie, R. Ansari, H. Rouhi, A numerical study on the buckling and vibration of nanobeams based on the strain and stress-driven nonlocal integral models, International Journal of Computational Materials Science and Engineering 7 (2018) 1850016.

[31] M. Fakher, Sh. Hosseini-Hashemi, Bending and free vibration analysis of nanobeams by differential and integral forms of nonlocal strain gradient with Rayleigh–Ritz method, Materials Research Express 4 (2017) 125025.

[32] H. Danesh, M. Javanbakht, M. Mohammadi Aghdam, A comparative study of 1D nonlocal integral Timoshenko beam and 2D nonlocal integral elasticity theories for bending of nanoscale beams, Continuum Mechanics and Thermodynamics (2021). https://doi.org/10.1007/s00161-021-00976-7

[33] M. Fazlali, S. A. Faghidian, M. Asghari, Nonlinear flexure of Timoshenko–Ehrenfest nano-beams via nonlocal integral elasticity, The European Physical Journal Plus 135 (2020) 638. https://doi.org/10.1140/epjp/s13360-020-00661-9

[34] M. Tuna, M. Kirca, Bending, buckling and free vibration analysis of Euler-Bernoulli nanobeams using Eringen's nonlocal integral model via finite element method, Composite Structures 179 (2017) 269-284.

[35] K. G. Eptaimeros, C. Chr. Koutsoumaris, G. J. Tsamasphyros, Nonlocal integral approach to the dynamical response of nanobeams, International Journal of Mechanical Sciences 115–116 (2016) 68-80.

[36] X. Zhu, Y. Wang, H.-H. Dai, Buckling analysis of Euler–Bernoulli beams using Eringen's two-phase nonlocal model, International Journal of Engineering Science 116 (2017) 130-140.

[37] R. Barretta, S. Ali Faghidian, F. Marotti de Sciarra, Stress-driven nonlocal integral elasticity for axisymmetric nano-plates, International Journal of Engineering Science 136 (2019) 38-52.

[38] A. Farajpour, C. Q. Howard, W. S. P. Robertson, On size-dependent mechanics of nanoplates, International Journal of Engineering Science 156 (2020) 103368.

[39] R. Barretta, M. Čanađija, F. Marotti de Sciarra, A. Skoblar, R. Žigulić, Dynamic behavior of nanobeams under axial loads: Integral elasticity modeling and size-dependent eigenfrequencies assessment, Mathematical Methods in the Applied Sciences, 2021. https://doi.org/10.1002/mma.7152

[40] R. Barretta, M. Čanađija, F. Marotti de Sciarra, On thermomechanics of multilayered beams, International Journal of Engineering Science 155 (2020) 103364.

[41] A. Francesco Russillo, G. Failla, G. Alotta, F. Marotti de Sciarra, R. Barretta, On the dynamics of nano-frames, International Journal of Engineering Science 160 (2021) 103433.

[42] A. C. Eringen, Linear theory of non-local elasticity and dispersion of plane waves, International Journal of Engineering Science 10 (1972) 425–435.

[43] J. N. Reddy, Nonlocal theories for bending, buckling and vibration of beams, International Journal of Engineering Science 45 (2007) 288-307.

[44] J. N. Reddy, Nonlocal nonlinear formulations for bending of classical and shear deformation theories of beams and plates, International Journal of Engineering Science 48 (2010) 1507-1518.

[45] J. Yang, L. L. Ke, S. Kitipornchai, Nonlinear free vibration of single-walled carbon nanotubes using nonlocal Timoshenko beam theory, Physica E: Low-dimensional Systems and Nanostructures 42 (2010) 1727-1735.

[46] S. C. Pradhan, T. Murmu, Small scale effect on the buckling analysis of single-layered graphene sheet embedded in an elastic medium based on nonlocal plate theory, Physica E: Low-dimensional Systems and Nanostructures 42 (2010) 1293-1301.

[47] H. Sarparast, A. Ebrahimi-Mamaghani, M. Safarpour, H. M. Ouakad, R. Dimitri, F. Tornabene, Nonlocal study of the vibration and stability response of small-scale axially moving supported beams on viscoelastic-Pasternak foundation in a hygro-thermal environment, Mathematical Methods in the Applied Sciences, 2020. https://doi.org/10.1002/mma.6859

[48] M. Arefi, Electro-mechanical vibration characteristics of piezoelectric nano shells, Thin-Walled Structures 155 (2020) 106912.

[49] M. Malikan, M. Krasheninnikov, V. A. Eremeyev, Torsional stability capacity of a nano-composite shell based on a nonlocal strain gradient shell model under a three-dimensional magnetic field, International Journal of Engineering Science 148 (2020) 103210.

[50] A. Rahmani, B. Safaei, Z. Qin, On wave propagation of rotating viscoelastic nanobeams with temperature effects by using modified couple stress-based nonlocal Eringen's theory, Engineering with Computers (2021). https://doi.org/10.1007/s00366-021-01429-0

[51] Y. Jiang, L. Li, Y. Hu, A nonlocal surface theory for surface–bulk interactions and its application to mechanics of nanobeams, International Journal of Engineering Science 172 (2022) 103624.

[52] X. Xu, B. Karami, M. Janghorban, On the dynamics of nanoshells, International Journal of Engineering Science 158 (2021) 103431.

[53] Sh. Dastjerdi, M. Malikan, R. Dimitri, F. Tornabene, Nonlocal elasticity analysis of moderately thick porous functionally graded plates in a hygro-thermal environment, Composite Structures 255 (2021) 112925.

[54] Sh. Dastjerdi, M. Malikan, B. Akgöz, Ö. Civalek, T. Wiczenbach, V. A. Eremeyev, On the deformation and frequency analyses of SARS-CoV-2 at nanoscale, International Journal of Engineering Science 170 (2022) 103604.

[55] I. Esen, A. A. Abdelrhmaan, M. A. Eltaher, Free vibration and buckling stability of FG nanobeams exposed to magnetic and thermal fields, Engineering with Computers (2021). https://doi.org/10.1007/s00366-021-01389-5

[56] Sh. Dastjerdi, B. Akgöz, On the statics of fullerene structures, International Journal of Engineering Science 142 (2019) 125-144.

[57] Sh. Dastjerdi, B. Akgöz, Ö. Civalek, On the effect of viscoelasticity on behavior of gyroscopes, International Journal of Engineering Science 149 (2020) 103236.

[58] M. Zamani Nejad, A. Hadi, Eringen's non-local elasticity theory for bending analysis of bi-directional functionally graded Euler–Bernoulli nano-beams, International Journal of Engineering Science 106 (2016) 1-9.

[59] H. M. Sedighi, A. Sheikhanzadeh, Static and Dynamic Pull-In Instability of Nano-Beams Resting on Elastic Foundation Based on the Nonlocal Elasticity Theory, Chinese Journal of Mechanical Engineering 30 (2017) 385–397.

[60] Y. Y. Zhang, Y. X. Wang, X. Zhang, H. M. Shen, G. L. She, On snap-buckling of FG-CNTR curved nanobeams considering surface effects, Steel and Composite Structures 38 (2021) 293-304.

[61] M. H. Dindarloo, L. Li, R. Dimitri, F. Tornabene, Nonlocal Elasticity Response of Doubly-Curved Nanoshells, Symmetry 12 (2020) 466.

[62] M. H. Jalaei, H.-T. Thai, Ö. Civalek, On viscoelastic transient response of magnetically imperfect functionally graded nanobeams, International Journal of Engineering Science 172 (2022) 103629.

[63] A. Farajpour, C. Q. Howard, W. S. P. Robertson, On size-dependent mechanics of nanoplates, International Journal of Engineering Science 156 (2020) 103368.

[64] M. S. Vaccaro, On geometrically nonlinear mechanics of nanocomposite beams, International Journal of Engineering Science 173 (2022) 103653.

[65] L. Li, R. Lin, Teng Y. Ng, Contribution of nonlocality to surface elasticity, International Journal of Engineering Science 152 (2020) 103311.

[66] H. Darban, R. Luciano, A. Caporale, F. Fabbrocino, Higher modes of buckling in shear deformable nanobeams, International Journal of Engineering Science 154 (2020) 103338.

[67] M. Sobhy, Thermoelastic Response of FGM Plates with Temperature-Dependent Properties Resting on Variable Elastic Foundations, International Journal of Applied Mechanics 7 (2015) 1550082.

[68] F. Ebrahimi, M. R. Barati, Hygrothermal effects on vibration characteristics of viscoelastic FG nanobeams based on nonlocal strain gradient theory, Composite Structures 159 (2017) 433-444.

[69] M. Tuna, M. Kirca, Exact solution of Eringen's nonlocal integral model for vibration and buckling of Euler–Bernoulli beam, International Journal of Engineering Science 107 (2016) 54-67.

[70] C. M. Wang, Y. Y. Zhang, S. S. Ramesh, S. Kitipornchai, Buckling analysis of micro- and nano-rods/tubes based on nonlocal Timoshenko beam theory, Journal of Physics D, 39 (2006) 3904–3909.

[71] M. Taghizadeh, H. R. Ovesy, S. A. M. Ghannadpour, Beam buckling analysis by nonlocal integral elasticity finite element method, International Journal of Structural Stability and Dynamics 16 (2016) 1550015-1–1550015-19.

Appendix A:

Pure elastic:

$$I_{11} = C_{11} \int_{-h/2}^{h/2} z^2 dz,$$

$$I_{13} = C_{11} \int_{-h/2}^{h/2} z f(z) dz,$$

$$I_{16} = G \int_{-h/2}^{h/2} \left(f'(z) \right)^2 dz,$$

$$I_{114} = C_{11} \int_{-h/2}^{h/2} \left(f(z) \right)^2 dz$$

Pure strain gradient:

$$I_{17} = g_{31} \int_{-h/2}^{h/2} dz,$$

$$I_{18} = g_{31} \int_{-h/2}^{h/2} f'(z) dz,$$

$$I_{116} = g_{31} \int_{-h/2}^{h/2} \left(f'(z) \right)^2 dz$$

Pure piezomagnetic:

$$I_{12} = \frac{q_{31}^2}{a_{33}} \int_{-h/2}^{h/2} z^2 dz,$$

$$I_{14} = \frac{q_{31}^2}{a_{33}} \int_{-h/2}^{h/2} z f(z) dz,$$

$$I_{112} = \frac{q_{31}^2}{a_{33}} \int_{-h/2}^{h/2} \left(f(z) \right)^2 dz,$$

$$I_{115} = \frac{q_{31} \psi}{h} \int_{-h/2}^{h/2} f(z) dz$$

Pure flexomagnetic:

$$I_{110} = \frac{f_{31}^2}{3a_{33}} \int_{-h/2}^{h/2} \left(3f'(z) - 2 \right) dz,$$

$$I_{111} = \frac{\psi f_{31}}{h} \int_{-h/2}^{h/2} dz,$$

$$I_{118} = \frac{f_{31}^2}{3a_{33}} \int_{-h/2}^{h/2} f'(z) \left(3f'(z) - 2 \right) dz,$$

$$I_{119} = \frac{\psi f_{31}}{h} \int_{-h/2}^{h/2} f'(z) dz$$

Piezomagnetic-flexomagnetic interaction:

$$I_{15} = \frac{f_{31} q_{31}}{a_{33}} \int_{-h/2}^{h/2} z f'(z) dz,$$

$$I_{19} = \frac{f_{31} q_{31}}{a_{33}} \int_{-h/2}^{h/2} f(z) dz,$$

$$I_{113} = \frac{f_{31} q_{31}}{3a_{33}} \int_{-h/2}^{h/2} \left[f(z) \left(3f'(z) - 2 \right) \right] dz,$$

$$I_{117} = \frac{f_{31} q_{31}}{a_{33}} \int_{-h/2}^{h/2} f(z) f'(z) dz$$

Appendix B:

Pure elastic:

$$I_{21}=C_{11}\int_{-h/2}^{h/2} z^2 dz,$$

$$I_{23}=C_{11}\int_{-h/2}^{h/2} zf(z)dz,$$

$$I_{26}=G\int_{-h/2}^{h/2} \left(f'(z)\right)^2 dz,$$

$$I_{214}=C_{11}\int_{-h/2}^{h/2} \left(f(z)\right)^2 dz$$

Pure strain gradient:

$$I_{27}=g_{31}\int_{-h/2}^{h/2} dz,$$

$$I_{28}=g_{31}\int_{-h/2}^{h/2} f'(z)dz,$$

$$I_{216}=g_{31}\int_{-h/2}^{h/2} \left(f'(z)\right)^2 dz$$

Pure piezomagnetic:

$$I_{22}=\frac{q_{31}^2}{a_{33}}\int_{-h/2}^{h/2} z^2 dz,$$

$$I_{24}=\frac{q_{31}^2}{a_{33}}\int_{-h/2}^{h/2} zf(z)dz,$$

$$I_{212}=\frac{q_{31}^2}{a_{33}}\int_{-h/2}^{h/2} \left(f(z)\right)^2 dz,$$

$$I_{215}=\frac{q_{31}\psi}{h}\int_{-h/2}^{h/2} f(z)dz$$

Pure flexomagnetic:

$$I_{210}=\frac{1}{3}f_{31}\left(\frac{f_{31}-h_{31}}{a_{33}}\right)\int_{-h/2}^{h/2}\left(3f'(z)-2\right)dz,$$

$$I_{211}=\frac{\psi f_{31}}{h}\int_{-h/2}^{h/2} dz,$$

$$I_{218}=\frac{f_{31}}{3}\left(\frac{f_{31}-h_{31}}{a_{33}}\right)\int_{-h/2}^{h/2} f'(z)\left(3f'(z)-2\right)dz,$$

$$I_{219}=\frac{\psi f_{31}}{h}\int_{-h/2}^{h/2} f'(z)dz,$$

$$I_{2111}=h_{31}\left(\frac{f_{31}-h_{31}}{a_{33}}\right)\int_{-h/2}^{h/2} zf''(z)dz,$$

$$I_{2114}=h_{31}\left(\frac{f_{31}-h_{31}}{a_{33}}\right)\int_{-h/2}^{h/2} f(z)f''(z)dz$$

Piezomagnetic-flexomagnetic interaction:

$$I_{25}=q_{31}\left(\frac{f_{31}-h_{31}}{a_{33}}\right)\int_{-h/2}^{h/2} zf'(z)dz,$$

$$I_{29}=\frac{f_{31}q_{31}}{a_{33}}\int_{-h/2}^{h/2} f(z)dz,$$

$$I_{213}=\frac{q_{31}}{3}\left(\frac{f_{31}-h_{31}}{a_{33}}\right)\int_{-h/2}^{h/2}\left[f(z)\left(3f'(z)-2\right)\right]dz,$$

$$I_{217}=\frac{f_{31}q_{31}}{a_{33}}\int_{-h/2}^{h/2} f(z)f'(z)dz,$$

$$I_{2110}=\frac{h_{31}q_{31}}{a_{33}}\int_{-h/2}^{h/2} zf'(z)dz,$$

$$I_{2112}=\frac{h_{31}q_{31}}{a_{33}}\int_{-h/2}^{h/2} f(z)dz,$$

$$I_{2113}=\frac{h_{31}q_{31}}{a_{33}}\int_{-h/2}^{h/2} f(z)f'(z)dz$$

$$I_{2115}=\frac{f_{31}q_{31}}{a_{33}}\int_{-h/2}^{h/2} zf'(z)dz$$

*The number of primes defines the number of derivatives. As an example, double prime $(\ )''$ means the second derivative with respect to *z*.

Appendix C:

$\alpha_1 = \int_0^{L_x} X_m \, X_m dx \, , \alpha_2 = \int_0^{L_x} X_m'' \, X_m dx \, ,$	$\beta_1 = \int_0^{L_x} X_m'' \, X_m' dx \, , \beta_2 = \int_0^{L_x} X_m''' \, X_m' dx \, ,$
$\alpha_3 = \int_0^{L_x} X_m''' \, X_m dx \, , \alpha_4 = \int_0^{L_x} X_m'''' X_m dx \, ,$	$\beta_3 = \int_0^{L_x} X_m'''' X_m' dx \, , \beta_4 = \int_0^{L_x} X_m''''' \, X_m' dx \, ,$
$\alpha_5 = \int_0^{L_x} X_m''''' \, X_m dx \, , \alpha_6 = \int_0^{L_x} X_m'''''' \, X_m dx$	$\beta_5 = \int_0^{L_x} X_m'''''' \, X_m' dx \, , \beta_6 = \int_0^{L_x} X_m''''''' \, X_m' dx$
*The number of primes defines the number of derivatives. As an example, the quadruple prime $(\,)''''$ means the fourth derivative with respect to *x*.	

Nomenclature:

ε_{xx} : Axial strain

γ_{xz} : Shear strain

η_{xxz} : Gradient of the axial elastic strain

C_{11} : Elastic modulus

G : Shear modulus

σ_{xx} : Axial stress

τ_{xz} : Shear stress

f_{31} : Component of the fourth-order flexomagnetic coefficients tensor

a_{33} : Component of the second-order magnetic permeability tensor

q_{31} : Component of the third-order piezomagnetic tensor

ξ_{xxz} : Component of the higher-order hyper-stress tensor

B_z : Magnetic flux

H_z : Component of magnetic field

W : Works performed by external forces

$\Re_1$ & $\Re_2$: Free energy

U : Strain energy

g_{31} : Influence of the sixth-order gradient elasticity tensor

u_i (i=1,3): Displacement in the x- and z- directions

u and w: Mid-plane's axial and lateral displacements

ϕ : Rotation of beam elements around the y-axis

z: Thickness coordinate

ψ : External magnetic potential

Ψ : Magnetic potential function

N_x^0: Axial in-plane force

N^0: Critical buckling load

Q_x : Shear stress resultant

M_x : Moment stress resultant

T_{xxz} : Hyper stress resultant

V_x, R_x : Higher-order stress resultants